

Chapter One

Introduction

(1-1) Importance of Temperature:

The temperature is the most important elements of climate that control of distribution of life on the earth's surface, it is also very important in controlling the direction of wind flow from low temperature to high temperature regions. Temperature also controls the types at plants growing in each region.

The Temperature difference is associated with the difference of the distribution of atmospheric pressure, which in turn controls the distribution of the wind and the associated movement of clouds and rainfall [1]. Thus the temperature is the most important element of climate that must be studied by researchers. The rain is the most important sources of water through feeding rivers and groundwater, as it contributes to irrigate large areas of farmland, and used for drinking to humans and animals [2].

Results from the sun that earth temperature gives heat and light when the sun sends the radiation to the earth's surface is through the atmosphere. Some at these radiations are reflected by the atmosphere and earth, while others are absorbed by them . The visible Radiation reaches the earths in different frequencies and in different wavelengths can be converted to heat energy by the earth surface [3].

(1-2) The Problem of The Thesis:

One can measure the temperature of the upper atmosphere by using balloons connected to Thermometers or sensors by using some software. [4] Such methods are expensive. Thus one must search for another way to measure the temperature of atmosphere layers by utilizing a new technique.

(1-3)Literature Review:

Attempts were made to relate temperature to spectrum of atoms, which simplify temperature determination. One of them is based on observing the spectrum of laser when temperature changes.[5]It was found that temperature increase, increase wavelength. In another work [6] the temperature decreases line width. In these attempts classical physical laws are used to explain spectrum sensitivity to temperature. This means that there is a need for quantum mechanical treatment which is suitable for describing atomic spectra.

(The Aim of The Thesis: 1-4 (

The aim is to find the temperature of different layers of the atmosphere by using simple methods such as spectral techniques. One needs to study how atomic spectra can respond to temperature. And to explain this on the basis of modified quantum and statistical laws.

(1-5)Thesis out line:

The thesis consist of four chapters .Chapter one is the introduction, and chapter two is concerned with atomic spectra .Chapter three is the literature review, while chapter four is devoted for contribution.

Chapter Two

Atmosphere and Atomic Spectra

(2-1) Introduction:

The spectrum of atoms is now widely used in many applications as a finger print characterizing the elements excited in samples. This comes from the fact that each element is characterized by certain specific energy levels. Thus each element emits photons due to transition between these energy levels. The energies and wavelengths of the photons emitted by a certain element is different from that emitted by all other elements

(2-2) Layer of The Atmosphere:

The [atmosphere](#) protects [life on earth](#) by absorbing [ultraviolet solar radiation](#), warming the surface through heat retention ([green house effect](#)), and reducing [temperature](#) extremes between [day](#) and [night](#).

Contains 78.08% [nitrogen](#), 20.95% [oxygen](#), 0.001% [neon](#), [carbon dioxide](#) 0.039% , and small amounts of other gases.

Earth's atmosphere can be divided (called atmospheric stratification) into five main layers. From highest to lowest, these layers are:

Exosphere, Thermosphere, Mesosphere, Stratosphere & Troposphere.
[7,8]

(2-2-1) [Exosphere](#)

The exosphere is the outermost layer of Earth's atmosphere. It extends from the [exobase](#), which is located at the top of the thermosphere at an altitude of about 500 km above sea level, to about 10,000 km .[9]

This layer is mainly composed of extremely low densities of hydrogen, helium and several heavier molecules including nitrogen, oxygen and carbon dioxide closer to the exobase.

(2-2-2) [Thermosphere](#)

The thermosphere is the second-highest layer of Earth's atmosphere. It extends from the mesopause (which separates it from the mesosphere) at an altitude of about 80 km up to the [thermopause](#) at an altitude range of 500–1,000 km. The height of the thermopause varies considerably due to changes in solar activity.

Since the thermopause lies at the lower boundary of the exosphere, it is also referred to as the [exobase](#). The lower part of the thermosphere, from 80 to 550 km above Earth's surface, contains the [ionosphere](#).

This atmospheric layer undergoes a gradual increase in temperature with height. Unlike the stratosphere, the inversion in the thermosphere occurs due to the extremely low density of its molecules. The temperature in this layer can be as high as 1,200 °C. [\[8, 9\]](#)

(2-2-3) [Mesosphere](#)

The mesosphere is the third highest layer of Earth's atmosphere, occupying the region above the stratosphere and below the thermosphere. It extends from the stratopause at an altitude of about 50 km (to the mesopause at 80–85 km)above sea level.

Temperatures drop with increasing altitude to the [mesopause](#) that marks the top of this middle layer of the atmosphere. It is the coldest place on Earth and has an average temperature around $-85\text{ }^{\circ}\text{C}$ ($-120\text{ }^{\circ}\text{F}$; 190 K). [\[9,10\]](#)

The mesosphere is also the layer where most [meteors](#) burn up upon atmospheric entrance. It is too high above Earth to be accessible to jet-powered aircraft and too low to support satellites and orbital or sub-orbital spacecraft. The mesosphere is mainly accessed by rocket-powered aircraft and unmanned sounding rockets. [11]

(2-2-4)[Stratosphere](#)

The stratosphere is the second-lowest layer of Earth's atmosphere. It lies above the troposphere and is separated from it by the [tropopause](#). This layer extends from the top of the troposphere at roughly 12 km above Earth's surface to the [stratopause](#) at an altitude of about 50 to 55 km, stratospheric temperatures range from -57°C to 0°C.

It contains the ozone layer, which is the part of Earth's atmosphere that contains relatively high concentrations of that gas.

The stratosphere defines a layer in which temperatures rise with increasing altitude. This rise in temperature is caused by the absorption of [ultraviolet radiation](#) (UV) radiation from the Sun by the [ozone layer](#), which restricts turbulence and mixing. Although the temperature may be -60 °C (-76 °F; 210 K) at the tropopause, the top of the stratosphere is much warmer, and may be near 0 °C.[11]

The stratospheric temperature profile creates very stable atmospheric conditions, so the stratosphere lacks the weather-producing air turbulence that is so prevalent in the troposphere. Consequently, the stratosphere is almost completely free of clouds and other forms of weather. However, polar stratospheric or [nacreous clouds](#) are occasionally seen in the lower part of this layer of the atmosphere where the air is coldest. [12]

(2-2-5)[Troposphere](#)

The troposphere is the lowest layer of Earth's atmosphere. It extends from Earth's surface to an average height of about 12 km, although this altitude actually varies from about 9 km at the poles to 17 km at the [equator](#),[\[14\]](#) with some variation due to [weather](#). The troposphere is bounded above by the [tropopause](#), a boundary marked by stable temperatures.

Although variations do occur, the temperature usually declines with increasing altitude in the troposphere because the troposphere is mostly heated through energy transfer from the surface. Thus, the lowest part of the troposphere is typically the warmest section of the troposphere. This promotes vertical mixing.

The troposphere is denser than all its overlying atmospheric layers because a larger atmospheric weight sits on top of the troposphere and causes it to be most severely compressed. Fifty percent of the total mass of the atmosphere is located in the lower 5.6 km (18,000 ft) of the troposphere. It is primarily composed of nitrogen (78%) and oxygen (21%) with only small concentrations of other trace gases.

Nearly all atmospheric water vapor or moisture is found in the troposphere, so it is the layer where most of Earth's weather takes place [\[13,15,16\]](#).

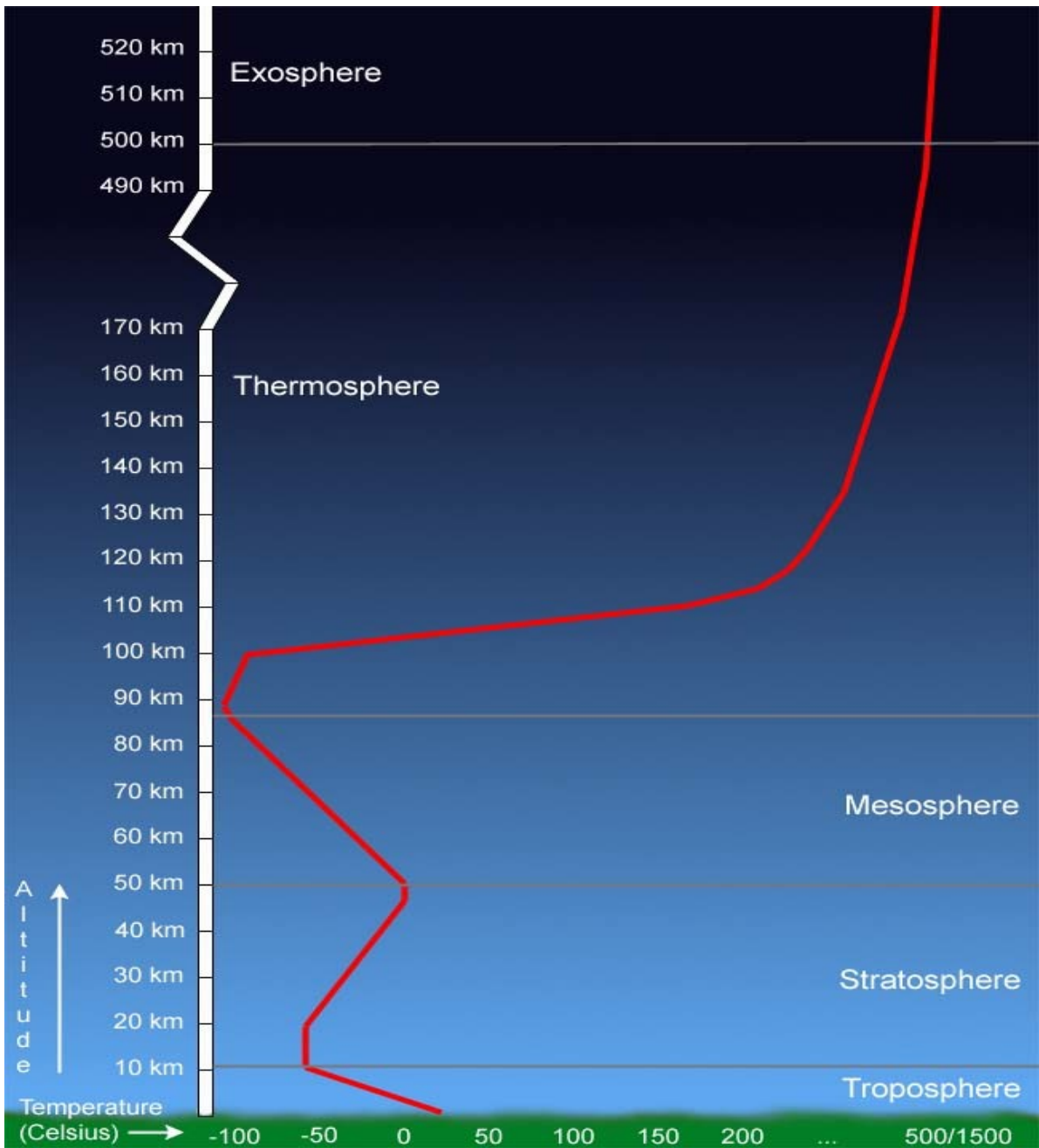


Fig (2-1) Layer of The Atmosphere[14].

(2-3) Gases in Atmosphere

(2-3-1) Butane (C_4H_{10})

The Butane components of natural gas can be removed by liquefaction and compressed into cylinders to be sold as bottled gas, which is used for fuel in many rural areas.[17]

(2-3-2) Carbon Monoxide (CO)

Carbon monoxide is formed when carbon is burned with a deficiency of oxygen, Carbon Monoxide is made industrially on a huge scale, together with hydrogen as synthesis gas and is used for a variety of large scale organic syntheses, although CO is an exceedingly weak Lewis base, one of its most important properties is the ability to act as a donor ligand toward transition metals.

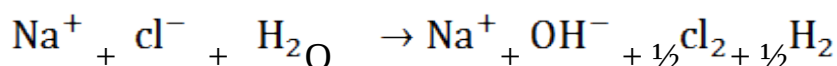
Carbon monoxide is very toxic, rapidly giving a bright red complex with the hemoglobin of blood. Carbon monoxide reacts with alkali metals in liquid ammonia to give alkali metal carbonyls [18].

(2-3-3) Carbon dioxide (CO_2)

Carbon dioxide an important green house gas, is obtained in combustion of carbon and hydrocarbons, calcinations of $CaCO_3$, it forms complexes with transition metals, the gas is very soluble in ethanol amines, while they are used to scrub carbon dioxide from gas streams[19,20].

(2-3-4) Chlorine (Cl_2)

Chlorine occurs in nature mainly as sodium chloride in seawater and in various inland salt lakes and as solid deposits originating presumably from the prehistoric evaporator of salt lakes, chlorine is prepared industrially mainly by electrolysis of brine[21]



Chlorine is greenish gas and moderately soluble in, but reactive with water.

(2-3-5) Fluorine (F_2)

Fluorine is more abundant in the earth crust (0.065%) than chlorine (0.055%) and forms concentrated deposits in such minerals as Fluorite, the element was first isolated in 1886 by Moissan, who pioneered the chemistry of fluorine and chlorine compounds, the yellow gas is obtained by electrolysis of HF [22].

(2-3-6) Nitrogen (N_2)

Nitrogen occurs in nature mainly as di nitrogen N_2 , an inter N_2 gas that comprises 78.1 by volume of the earth's atmosphere. No other allotrope except nitrogen is known or likely to be, although the possible stability of many others, N_3N_4 , N_5 has been examined Theoretically.[23]

(2-3-7) Neon (Ne)

Neon is the second-lightest noble gas, its color is reddish-orange in a vacuum discharge tube and in neon lamps. The refrigerating capacity of helium is over 40 times the one of liquid [helium](#) and three times that of liquid [hydrogen](#) (on a per unit volume basis). It is a less expensive refrigerant than helium in most applications.

(2-3-8) Oxygen (O_2)

Oxygen is a [chemical element](#) with symbol O and [atomic number](#) 8.

Oxygen gas is the second most common component of the [Earth's atmosphere](#), taking up 20.8% of its volume [23]

A simplified overall formula for photosynthesis is:



Or simply: [carbon dioxide](#) + water + sunlight \rightarrow [glucose](#) + dioxygen

(2-4)The Ordinary Schrödinger Equation:

(2-4-1) The Time-Dependent Schrödinger Equation:

The Schrödinger equation is the key equation of quantum mechanics. this second order, partial differential equation determines the spatial shape and temporal evolvment of a wave function in a given potential and for given boundary conditions. The one-dimensional Schrödinger equation is used when the particle of interest is confined to one spatial dimension .to derive the one-dimensional Schrödinger equation, we start with the total energy equation, i.e. the sum of kinetic and potential energy.[24,25,26]

$$\frac{p^2}{2m} + U(x) = E_{total} \quad (2-4-1)$$

$$P = \hbar K , \quad E = \hbar\omega$$

An operator

$$i \frac{\partial}{\hbar \partial t} = \hat{E} \quad (2-4-2)$$

$$-i \frac{\partial}{\hbar \partial x} = \hat{P} \quad (2-4-3)$$

Substitution of the dynamical variables by their quantum mechanical operators which act on the wave functions $\Psi(x, t)$ yields the one-dimensional time dependent Schrödinger equation:

$$-\frac{\hbar^2}{2m} \frac{\partial^2}{\partial x^2} \Psi(x, t) + U(x) \Psi(x, t) = -\frac{\hbar}{i} \frac{\partial}{\partial t} \Psi(x, t) \quad (2-4-4)$$

The left side of this equation can be rewritten by using Hamiltonian operator or total energy [27,28, 29]

$$H = -\frac{\hbar^2}{2m} \frac{\partial^2}{\partial x^2} + U(x) \quad (2-4-5)$$

hence the time dependent Schrödinger equation can be written as:

$$H\Psi(x, t) = -\frac{\hbar}{i} \frac{\partial}{\partial t} \Psi(x, t) \quad (2-4-6)$$

Since The Schrödinger equation is partial differential equation, the method can be used to separate the equation into spatial and a temporal part. [32,31,30]

$$\Psi(x, t) = \Psi(x) f(t) \quad (2-4-7)$$

Where $\Psi(x)$ depend only on x and $f(t)$ depend only on t .

Insertion of Eq. (2-4-7) into the Schrödinger equation yields

$$\frac{1}{\Psi(x)} H\Psi(x) = \frac{i\hbar}{f(t)} \frac{d}{dt} f(t) \quad (2-4-8)$$

The left side of this equation depends on x only, while the right side depends on t , because x and t are completely independent variables, the equation can be true only if both sides are constants

$$\frac{i\hbar}{f(t)} \frac{d}{dt} f(t) = \text{const} \quad (2-4-9)$$

Tentatively this constant is designated as $\text{const} - E$ where the meaning of E become evident below, integration of Equation (2-4-9) yields

$$f(x) = e^{-iEt/\hbar} \quad (2-4-10)$$

Insertion of this result in to Equation (2-4-7) yields the time-dependent wave function

$$\Psi(x, t) = \Psi(x)e^{-iEt/\hbar} \quad (2-4-11)$$

If E is real, then the wave function has amplitude $\Psi(x)$ and a phase $\exp(-iEt/\hbar)$. The amplitude and a phase representation are convenient for many applications. To find the physical meaning of the real quantity E , we calculate expectation value of the total energy using the wave function obtained from the product method [34,33,26]

$$E_{total} = e^{iEt/\hbar} e^{-iEt/\hbar} E \int_{-\infty}^{\infty} \Psi^*(x)\Psi(x)dx = E \quad (2-4-12)$$

Because the wave function is normalized that is

$$\langle \Psi(x), \Psi(x) \rangle = 1 \quad (2-4-13)$$

The designated as E the expectation value of the total energy.[35,36]

(2-4-2) The Time-Independent Schrödinger Equation

The time-independent Schrödinger equation is obtained by inserting the wave function obtained from the product method .Equation (2-4-11) into the time-independent Schrödinger equation one obtains

$$-\frac{\hbar^2}{2m} \frac{\partial^2}{\partial x^2} \Psi(x) + U(x)\Psi(x) = E\Psi(x) \quad (2-4-14)$$

This is the time-independent Schrödinger equation. Using the Hamiltonian operator, one obtains

$$H \Psi(x) = E\Psi(x) \quad (2-4-15)$$

Since H is an operator and E is real number, the Schrödinger equation has the form of an eigenvalue equation. The Eigen Function $\Psi_n(x)$ and the eigenvalue E_n are found by solving the Schrödinger equation.

The eigenvalue of the Schrödinger equation E_n are discrete, that is only certain energy values are allowed, all other energies are disallowed or forbidden. The energy eigenvalues or Eigen energies. The lowest Eigen state energy is ground state energy. All higher energies are called of excited state energies.[37]

(2-4-3)Probability Current Density

The Probability Current Density is given by

$$\begin{aligned} \frac{\partial}{\partial t} \int p d^3r &= \int \frac{\partial |\Psi|^2}{\partial t} d^3r = \int \frac{\partial}{\partial t} \Psi^* \Psi d^3r \\ &= \int \left[\Psi^* \frac{\partial \Psi}{\partial t} + \frac{\partial \Psi^*}{\partial t} \Psi \right] d^3r \end{aligned} \quad (2-4-16)$$

But from Schrödinger equation

$$\frac{i\hbar \partial \Psi}{\partial t} = \frac{-\hbar^2}{2m} \nabla^2 \Psi + U\Psi \quad , \quad \frac{-i\hbar \partial \Psi^*}{\partial t} = \frac{-\hbar^2}{2m} \nabla^2 \Psi^* + U\Psi^*$$

$$\frac{\partial \Psi}{\partial t} = \frac{-i\hbar^2}{2m} \nabla^2 \Psi - iU\Psi \quad , \quad \frac{\hbar \partial \Psi^*}{\partial t} = \frac{-i\hbar^2}{2m} \nabla^2 \Psi^* + iU\Psi^*$$

(2-4-17)

Thus

$$\begin{aligned} \frac{\partial}{\partial t} \int p d^3r &= \frac{i\hbar}{2m} \int \Psi^* \nabla^2 \Psi - \Psi \nabla^2 \Psi^* d^3r \\ &= \frac{i\hbar}{2m} \int \nabla \cdot [\Psi^* \nabla \Psi - (\nabla \Psi^*) \Psi] d^3r \\ &= \frac{i\hbar}{2m} \int \nabla \cdot S d^3r = \frac{i\hbar}{2m} \int \nabla \cdot [\Psi^* \nabla \Psi - (\nabla \Psi^*) \Psi] dA \end{aligned} \quad (2-4-18)$$

But the continuity equation reads

$$\frac{\partial \rho}{\partial t} + \nabla \cdot J = 0 \quad (2-4-19)$$

In view of (2-4-18)

$$\frac{\partial \rho}{\partial t} + \nabla \cdot S = 0 \quad (2-4-20)$$

Thus S represents the Intensity of particles, i .e the flux of particles

Crossing unit area per unit time, where

$$S = \frac{i\hbar}{2m} [\Psi^* \nabla \Psi - \Psi (\nabla \Psi^*)] \quad (2-4-21)$$

It is well known that the momentum operator is hermition .Hence

$$\int \widehat{P} \overline{\Psi} \Psi d^3r = \int \overline{\Psi} \widehat{P} \Psi d^3r$$

$$-\frac{\hbar}{i} \int \nabla \Psi^* \Psi d^3r = -\frac{\hbar}{i} \int \Psi^* \nabla \Psi d^3r$$

Hence

$$\Psi \nabla \Psi^* = -\Psi^* \nabla \Psi$$

Therefore

$$S = \frac{i\hbar}{2m} [2\Psi^* \nabla \Psi]$$

$$S = \frac{i\hbar}{m} \Psi^* \nabla \Psi \quad (2-4-22)$$

Generally =Real $\left[\frac{i\hbar}{m} \Psi^* \nabla \Psi \right]$

(2-5) Maxwell- Boltzmann Distribution

In order to derive Maxwell- Boltzmann distribution one must first find a general expression of (W) which represents the number of different ways in which the molecules can be arranged among the cells in phase space. The most probable distribution is therefore the one for which (W) is maximum. One can assume that each cell in phase space is equally likely to be occupied.[38,39,40]

If there are g_i cells with the every E_i the number of ways in which one molecules can have energy E_i is g_i . The total number of ways that n_i molecules can have the energy E_i is $g_i^{n_i}$.

hence the number of ways in which all N molecules can be distributed among the various is product of factors of the form $g_i^{n_i}$ such as

$$(g_i^{n_1}) \cdot (g_i^{n_2}) \cdot (g_i^{n_3}) \dots (g_i^{n_i}) \quad (2-5-1)$$

The total number of permutation possible for N molecules is $N!$, but we must divide it by irrelevant permutations, which are

$$\frac{n_1! n_2! n_3! \dots}{N!} \quad (2-5-2)$$

Where

$$N = \sum n_i = n_1 + n_2 + n_3 + \dots \quad (2-5-3)$$

The total number of ways in which the molecule can be distributed among possible energy levels is product of equation (2-5-1) (2-5-2);

$$W = \frac{N!}{n_1! n_2! n_3!} g_1^{n_1} \cdot g_2^{n_2} \cdot g_3^{n_3} \quad (2-5-4)$$

To find the maximum value for W , which usually occurs at upper limit, it is important to express W in terms of n_i because $n_i!$ has no derivation. One can use Sterling formula, to eliminate $n_i!$ where;

$$\ln n! = n \ln n - n + 1 \quad (2-5-5)$$

Since the numbers of molecules are large, thus $n \gg 1$ and equation (2-5-5) becomes;

$$\ln n! = n \ln n - n \quad (2-5-6)$$

The value of W is directly proportion to $\ln W$. Since $\ln W$ is in upper limit. And then W is also in upper limit. [41]

The natural logarithm of equation (2-5-4) is;

$$\ln W = \ln N! - \sum \ln n_i! + \sum n_i \ln g_i \quad (2-5-7)$$

By using Sterling's formula equation (2-5-6) becomes; (2-5-6)

$$N = \sum n_i$$

Since;

$$\ln W = N \ln N - \sum n_i \ln n_i + \sum n_i \ln g_i \quad (2-5-8)$$

In upper limit;

$$\frac{\partial \ln W}{\partial n_i} = 0 \quad (2-5-9)$$

Hence;

$$\partial \ln W = \sum n_i \partial \ln n_i - \sum \ln n_i \partial n_i + \sum \ln n_i \partial g_{i=0} \quad (2-5-10)$$

Since the total number of molecules in the system is constant then from (2-5-3);

$$\sum \partial n_{i=0} \quad (2-5-11)$$

And

$$\partial \ln n_i = \frac{1}{n_i} \partial n_i$$

$$\sum n_i \partial \ln n_i = \sum \partial n_{i=0} \quad (2-5-12)$$

$$- \sum \ln n_i \partial n_i + \sum \ln g_i \partial n_{i=0}$$

$$- \alpha \sum \partial n_{i=0} \quad (2-5-14)$$

The total energy of molecules in the system is constant hence;

$$\sum n_i \epsilon_i = E$$

$$\sum \varepsilon_i \partial n_i = \partial E = 0 \quad (2-5-15)$$

Multiplying equation (2-5-15) by $(-\beta)$

$$-\beta \sum \varepsilon_i \partial n_i = 0 \quad (2-5-16)$$

Where α and β are called Lagrange's factor.

To satisfy the distribution law one must add equations (2-5-13, 14, 16) to get:

$$-\sum(-\ln n_i + \ln g_i - \alpha - \beta \varepsilon_i) dn_{i=0} \quad (2-5-17)$$

In order for equations (2-5-17) to be true, then the quantity within the brackets must be zero for each value of n_i hence:

$$-\ln n_i + \ln g_i - \alpha - \beta \varepsilon_{i=0} \quad (2-5-18)$$

$$\ln n_i = \ln g_i - \alpha - \beta \varepsilon_i$$

$$n_i = g_i e^{-\alpha - \beta \varepsilon_i} \quad (2-5-19)$$

The last expression is known as Maxwell-Boltzmann distribution law.

(2-6)Line-Width Broadening

Lines the natural shape of an emission line appears under ideal conditions when the emitting atom is at rest and is not subject to the action of any external forces during the process of emission. In practice, ideal conditions are never realized completely because it is interactions with other atoms. These circumstances generally affect the shape of the emission line. Hence the natural shape of line is usually not observed under actual conditions.[42]

The broadening of emission can be divided into two groups:

1- Uniform broadening: which cause the same variation in the emission line of each atom.

2-Non-uniform broadening: cause difference types of variation in the emission line of individual atoms.

The natural width of emission line is an example of uniform broadening of lines since this broadening is the same in the emission lines of all atoms of given species and determined only by the emission time . The observable shape of the emission line for a set of atoms coincides with shape of the emission line for an individual atom.

(2-7)Collision Broadening

To calculate the collision broadening one can assume that the natural width of the emission line is equal to zero. Since the collision is random, the time between successive collisions obeys Poisson's distribution, i.e. in

the interval between $\bar{E}E$ [43,44]

$$P(\xi) d\xi = (1/\tau_0) \exp(-\xi/\tau_0) d\xi \quad (2-7-1)$$

$\tau_0 =$ is the mean time between collisions

The electric field strength of the emitted is practically given by:

$$E(t) = E_0 \exp(i\omega_0 t + i\phi) \quad (2-7-2)$$

$\phi =$ is a random phase

Where for sufficiently very long time the average field intensity is given to be:

$$E_\omega = \int_{-x}^x E(t) e^{i\omega t} dt \quad (2-7-3)$$

The spectral composition of the emissive power $W(\omega)$ is given by the intensity relation:

$$W(\omega) \propto E_\omega E_\omega^* = \frac{E_0^2}{4} \frac{\sin^2 [(\omega_0 - \omega)\xi/2]}{(\omega_0 - \omega)^2} \quad (2-7-4)$$

This equation describes the intensity of radiation from an individual atom over an interval of time ξ and the spectral intensity of the total radiation from all atoms takes the form

$$W(\omega) = \frac{1}{2} \frac{1}{(\omega_0 - \omega)^2 + (\frac{1}{\tau_0})^2} \quad (2-7-5)$$

The maximum value of W is

$$W_m = \frac{\tau_0^2}{2} \quad \text{at } \omega = \omega_0$$

At half maximum

$$\frac{1}{2} W_m = \frac{\tau_0^2}{4} \quad (2-7-6)$$

This means that the collision broadening leads to the Lorentz shape of line with a width.

(2-8) Doppler Broadening:

If an atom is moving during the emission process, the frequency of the radiation emitted by it is not equal to the frequency of radiation emitted by an atom at rest. The laws of conservation of the energy and momentum for a radiating atom have the form;

$$E_2 + (1/2)Mv_2^2 = E_1 + (1/2)Mv_1^2 + \hbar\omega \quad (2-8-1)$$

$$Mv_2 = Mv_1 + \hbar k \quad (2-8-2)$$

Where E_2 the energy of the excited state of the atoms, E_1 is the energy of the low level which the emitting electron undergoes, M is the mass of the atom

v_2, v_1 represent the electron velocities before and after the act of emission. While $\hbar\omega$ and $\hbar k$ are the energy and the momentum of the emitted photon. If transition takes place from level E_2 to E_1 , hence

$$\hbar\omega_0 = E_2 - E_1 \quad (2-8-3)$$

Consider atom at the energy level E_2 moving with velocity v_2 , emits a photon of energy $\hbar\omega$, then its energy becomes E_1 , while its velocity changes to v_1 . thus according to the principle of energy and momentum conservation one gets:

$$E_2 + (1/2)Mv_2^2 = E_1 + (1/2)Mv_1^2 + \hbar\omega$$

In view of equation(2-8-3)one gets

$$\hbar(\omega_0 - \omega) = \hbar\omega^2/(2Mc^2) - \omega v_2/c \quad (2-8-4)$$

hence

$$\omega = \frac{\omega_0}{1-(v_2/c)} \approx \omega_0 \left(1 + \frac{v_2}{c}\right) \quad (2-8-5)$$

This formula describe the Doppler effects in the direction of the velocity of the atom ,the frequency of the emitted photon increases by

$\Delta\omega = \frac{v_2\omega_0}{c}$, while the frequency of the photon emitted in the opposite

direction decreases by same amount.

From Maxwell's distribution, the number of atoms having velocities between v_2 and $v_2 + dv_2$ is proportional to

$$n(v_2) = dv_2 \exp[-Mv_2^2/(2kT)] \quad (2-8-6)$$

Where k is Boltzmann constant.

From (2-8-5) one obtains

$$v_2 = (\omega - \omega_0)c/\omega_0 \quad , dv_2 = (c/\omega_0)d\omega$$

The frequency distribution of the radiated energy is given by:

$$W(\omega)d\omega = \exp\left[\frac{-Mc^2(\omega-\omega_0)^2}{(2\omega_0^2kT)}\right]d\omega \quad (2-8-7)$$

Hence the spectral width is given by

$$\Delta\omega = 2\omega_0[2kT \ln 2 (Mc^2)]^{1/2} \quad (2-8-8)$$

It is convenient to present Gaussian distribution in the form

$$F_G(\omega) = [1/\sigma\sqrt{2\pi}] \exp[-(\omega - \omega_0)^2/(2\sigma^2)] \quad (2-8-9)$$

where

$$\sigma = [kT\omega_0^2/(Mc^2)]^{1/2} \quad (2-8-10)$$

The Gaussian distribution is normalized to unity:

$$\int_{-x}^x F_G(\omega)d\omega = 1 \quad (2-8-11)$$

The shape of a composite emission line when an emission line undergoes broadening due to the simultaneous action of several factors.

The resultant line is connected with the component through that all the lines have the same center frequency (ω_0), if $F_1(\omega)$ and $F_2(\omega)$ characterize two emission lines with the same central frequency (ω_0) the shape of the composite emission line is defined as follow

$$F(\omega) = \int_{-\infty}^{\infty} F_1(\xi)F_2(\omega + \omega_0 - \xi)d\xi \quad (2-8-12)$$

Chapter Three

Literature Review

(3-1) Introduction

Ordinary statistical law can successfully describe a wide variety of physical phenomena. But unfortunately it is not capable of describing some physical phenomena associated with super conductors, like the specific heat capacity. Moreover, it cannot account for the effect of magnetic energy. For instance, if the material is magnetized, its magnetization does not change the potential and kinetic energy.

This work is concerned with deriving statistical laws from plasma equations and simple quantum treatment to incorporate frictional, magnetic, and other field energies in the statistical laws. It also derives

Gibbs distribution, besides deriving the effect of fields from plasma as well as the ordinary statistical expression of average energy [45].

(3-2) Derivation of Statistical Laws From Plasma Equation

The plasma equation of motion of particles in the presence of a field potential per particle V and a pressures force P beside a resistive force F_r is given by;[45]

$$nm \frac{dv}{dt} = -\nabla p - Fr - \nabla nV \quad (3-2-1)$$

Where n, m stands for particle number density and particle mass respectively considering the motion to be in one dimension along the x -axis the equation of motion becomes;

$$nm \frac{dv}{dx} \frac{dx}{dt} = -\frac{dp}{dx} - \frac{d(nV)}{dx} - F_r$$

$$(3-2-2) \quad nmv \frac{dv}{dx} = -\frac{dp}{dx} - \frac{d(nV)}{dx} - F_r$$

(3-2-3)

The term T stands for the kinetic energy at a single particle and can be written as;

$$T = \frac{1}{2} mv^2 = E_0 \quad (3-2-4)$$

The pressure P can also split in to thermal P_t and non-thermal P_0 to be in the form ;

$$P = P_t + P_0 = nkT + nP_p \quad (3-2-5)$$

Where P_p the non-thermal pressure for one particle.

(3-2-1) Plasma Statistical Equation in the Presence of Potential Field Only

When the potential is only present beside the thermal pressure term the equation of motion (3-2-3) read;

$$n \frac{dE_0}{dx} = - \frac{d(nV)}{dx} - \frac{d(nkT)}{dx}$$

(3-2-6)

If one assumes p_t to change with (X) due to the change of (n) only then equation (3-2-6) to;

$$n \frac{dE_0}{dx} = -kT \frac{dn}{dx} - \frac{d(nV)}{dx} \quad (3-2-7)$$

The temperature here is assumed to be uniform; here one has two cases either $V_T = nV$ changes with respect to X due to the change of V only .

In this case equation (3-2-7) reads;

$$n \frac{dE_0}{dx} = -kT \frac{dn}{dx} - n \frac{dV}{dx} \quad (3-2-8)$$

$$n \frac{d(E_0 + V)}{dx} = -kT \frac{dn}{dx} \quad (3-2-9)$$

The total energy is given by;

$$E = T + V = E_0 + V \quad (3-2-10)$$

Therefore (3-2-9) becomes;

$$n \frac{dE}{dx} = -kT \frac{dn}{dx}$$

$$ndE = -kT dn$$

Integration both sides yields;

$$-\int \frac{dE}{kT} = \int \frac{dn}{n}$$

$$\ln n = -\frac{E}{kT} + C_0$$

$$n = C e^{\frac{-E}{kT}} \quad (3-2-11)$$

This is the ordinary Maxwell-Boltzmann distribution. But if V_T changes

due to change of (n) only, then equation (3-2-7) reads;

$$n \frac{dE_0}{dx} = -kT \frac{dn}{dx} - V \frac{dn}{dx}$$

$$n \frac{dE_0}{dx} = -(kT + V) \frac{dn}{dx}$$

$$-\frac{dE_0}{(kT + V)} = \frac{dn}{n}$$

Integration both sides yields;

$$\int \frac{dn}{n} = - \int \frac{dE_0}{(kT + V)}$$

$$\ln n = - \frac{E_0}{kT + V} + C_0$$

$$n = C_0 e^{\frac{-E_0}{(kT+V)}} \quad (3-2-12)$$

The energy E_0 here stands for the kinetic energy only as shown by equation (3-2-4).

(3-2-2) Plasma Statistical Equation When Thermal Pressure Changes Due to the Temperature Changes

When the thermal pressure change due to the temperature change;

$$\frac{dP_t}{dx} = n \frac{d(kT)}{dx} \quad (3-2-13)$$

In this case the plasma equation (3-2-3) in the absence of a resistive force is given by;

$$n \frac{dE_0}{dx} = - \frac{dp_t}{dx} - \frac{d(nV)}{dx}$$

$$n \frac{dE_0}{dx} = -n \frac{d(kT)}{dx} - \frac{d(nV)}{dx} \quad (3-2-14)$$

Where the pressure here is assumed to be due to the thermal pressure only. If the total potential V_T is assumed to be related to the rate of change at V only, i.e.

$$\frac{dV_T}{dx} = \frac{d(nV)}{dx} = n \frac{dV}{dx} \quad (3-2-15)$$

In this case equation (3-2-14) reads;

$$n \frac{dE_0}{dx} = -n \frac{d(kT)}{dx} - n \frac{dV}{dx}$$

$$E_0 = -kT - V + C_0$$

Thus;

$$C_0 = E_0 + kT + V$$

One can easily deduce that C_0 is equal to the total energy E , i.e.

$$E = E_0 + V + kT \quad (3-2-16)$$

i.e. the total energy is equal to kinetic energy E_0 beside potential energy

V and thermal energy kT .

But if V_T change due to the rate of change of n only, i.e.

$$\frac{dV_T}{dx} = V \frac{dn}{dx} \quad (3-2-17)$$

Equation (3-2-14) thus reads;

$$\begin{aligned} n \frac{dE_0}{dx} &= -n \frac{d(kT)}{dx} - kT \frac{dn}{dx} - n \frac{dV}{dx} \\ n(dE_0 + d(kT) + dV) &= -kT dn \\ \int \frac{dn}{n} &= - \int \frac{(dE_0 + d(kT) + dV)}{kT} \\ \ln n &= - \frac{(E_0 + kT + V)}{kT} + C_0 \\ n &= C e^{\frac{-(E_0 + kT + V)}{kT}} \end{aligned} \quad (3-2-18)$$

If the change of V_T with respect to (X) is due to the change of both (n) and (V) with respect to (X);

$$\frac{dV_T}{dx} = \frac{d(nV)}{dx} = n \frac{dV}{dx} + V \frac{dn}{dx} \quad (3-2-19)$$

;Inserting (3-2-19) in (3-2-14) yields

$$\begin{aligned} n \frac{dE_0}{dx} &= -n \frac{d(kT)}{dx} - kT \frac{dn}{dx} - V \frac{dn}{dx} \\ n(dE_0 + d(kT)) &= -(kT + V) dn \\ \frac{dn}{n} &= - \frac{(dE_0 + d(kT))}{(kT + V)} \end{aligned}$$

$$\int \frac{dn}{n} = - \int \frac{(dE_0 + d(kT))}{(kT + V)}$$

$$\ln n = - \frac{(E_0 + kT)}{(kT + V)} + C_0$$

$$n = C e^{\frac{-(E_0 + kT)}{(kT + V)}}$$

(3-2-20)

Thus for non-uniform temperature systems, and non-uniform potential energy per particle, the statistical distribution law is described by (3-2-20). This relation is different from that obtained in (3-2-11), where the temperature is assumed to be uniform.

(3-2-3) Plasma Statistical Equation When Thermal Pressure Change

Due to the Change of Both (n) and (T)

When the thermal pressure changes due to the change of both (n) and (T), in this case the plasma equation (3-2-14) is given by ;

$$n \frac{dE_0}{dx} = -n \frac{d(kT)}{dx} - kT \frac{dn}{dx} - \frac{d(nV)}{dx} \quad (3-2-21)$$

If the total potential V_T is assumed to be related to the rate of change of (V) only ,i.e.

$$\frac{dV_T}{dx} = \frac{d(nV)}{dx} = n \frac{dV}{dx} \quad (3-2-22)$$

In this case equation (3-2-21) reads;

$$\begin{aligned} n \frac{dE_0}{dx} &= -n \frac{d(kT)}{dx} - kT \frac{dn}{dx} - n \frac{dV}{dx} \\ n(dE_0 + d(kT) + dV) &= -kT dn \\ \int \frac{dn}{n} &= - \int \frac{(dE_0 + d(kT) + dV)}{kT} \\ \ln n &= - \frac{(E_0 + kT + V)}{kT} + C_0 \\ n &= C e^{\frac{-(E_0 + kT + V)}{kT}} \end{aligned} \quad (3-2-23)$$

But if V_T change due to the rate of change on n only , I.e

$$\frac{dV_T}{dx} = \frac{d(nV)}{dx} = V \frac{dn}{dx} \quad (3-2-24)$$

In this case equation (3-2-21) reads;

$$\begin{aligned} n \frac{dE_0}{dx} &= -n \frac{d(kT)}{dx} - kT \frac{dn}{dx} - V \frac{dn}{dx} \\ n(dE_0 + d(kT)) &= -(kT + V) dn \\ \frac{dn}{n} &= - \frac{(dE_0 + d(kT))}{(kT + V)} \\ \int \frac{dn}{n} &= - \int \frac{(dE_0 + d(kT))}{(kT + V)} \end{aligned}$$

$$\ln n = -\frac{(E_0 + kT)}{(kT + V)} + C_0$$

$$n = C e^{\frac{-(E_0 + kT)}{(kT + V)}} \quad (3-2-25)$$

If the change of V_T with respect to (X) is due to the change of both n and V with respect to (X), then ;

$$\frac{dV_T}{dx} = \frac{d(nV)}{dx} = n \frac{dV}{dx} + V \frac{dn}{dx} \quad (3-2-26)$$

Inserting equation (3-2-26) in (3-2-21) yields;

$$n \frac{dE_0}{dx} = -n \frac{d(kT)}{dx} - kT \frac{dn}{dx} - n \frac{dV}{dx} - V \frac{dn}{dx}$$

$$n(dE_0 + dV + d(kT)) = -(kT + V)dn$$

$$\int \frac{dn}{n} = - \int \frac{(dE_0 + dV + d(kT))}{(kT + V)}$$

$$\ln n = -\frac{(E_0 + kT + V)}{(kT + V)} + C_0$$

$$n = C e^{\frac{-(E_0 + kT + V)}{(kT + V)}} \quad (3-2-27)$$

(3-2-4) Statistical Distribution Law from the Plasma Equation in the Presence of Friction

The plasma equation (3-2-3) can be written when only thermal pressure and frictional force acts in the form;

$$n \frac{dE_0}{dx} = -kT \frac{dn}{dx} - nF_r \quad (3-2-28)$$

Where F_r is the frictional force per particle.

Multiplying both sides by dx , one gets;

$$n dE_0 = -kT dn - n F_r \cdot dx \quad (3-2-29)$$

$$n(dE_0 + F_r \cdot dx) = -kT dn$$

$$\frac{dn}{n} = -\frac{1}{kT} (dE_0 + F_r \cdot dx)$$

$$\int \frac{dn}{n} = -\frac{1}{kT} \left(\int dE_0 + \int F_r \cdot dx \right)$$

$$\ln n = -\frac{1}{kT} (E_0 + \int F_r \cdot dx) + C_0$$

$$n = C e^{\frac{-(E_0 + \int F_r \cdot dx)}{(kT)}} \quad (3-2-30)$$

Thus the number of particles n having energy E_0 and subjected to a frictional force F_r is given by (3-2-30).

(3-2-5) Statistical Distribution When Chemical Potential is Present

Consider the plasma equation in which the particles are affected by the force (F) beside the thermal pressure (p_{th}).

The equation of motion in this case becomes

$$nm \frac{dv}{dt} = F - \frac{dp_{th}}{dx} \quad (3-2-31)$$

This equation can be rewritten to eliminate (t) in the form;

$$\begin{aligned} nm \frac{dv}{dx} \cdot \frac{dx}{dt} &= F - \frac{dp_{th}}{dx} \\ nmv \frac{dv}{dx} &= F - \frac{dp_{th}}{dx} \\ n \frac{dE_0}{dx} &= F_1 + F_2 - kT \frac{dn}{dx} \end{aligned} \quad (3-2-32)$$

F_1 is the force exerted on the system by pressure.

In thermodynamics the work done by the system is;

$$dW_T = -F_T dx \quad (3-2-33)$$

But F_T is the force exerted by the system. Thus the force exerted on the system F_1 related to F_T according to the relation;

$$dW_T = -F_1 dx$$

$$F_1 = - \frac{dW_T}{dx} \quad (3-2-34)$$

Inserting (3-2-34) in (3-2-32) yields;

$$n \frac{dE_0}{dx} = - \frac{dW_T}{dx} - kT \frac{dn}{dx} + F_2 \quad (3-2-35)$$

The total work can be written in terms of the work (W) per unit particle in the form;

$$n \frac{dE_0}{dx} = -n \frac{dW}{dx} - kT \frac{dn}{dx} + F_2 \quad (3-2-36)$$

The addition of new particles to the system corresponds to the force F_2 ;

$$dW_{ch} = F_2 dx \quad (3-2-37)$$

$$dW_{ch} = -dV_{ch} \quad (3-2-38)$$

$$V_{ch} = -\mu Nn \quad (3-2-39)$$

Where μ represents the binding energy which is negative. If one considers the change of V_{ch} due to the change of the change of μN only then;

$$dV_{ch} = -nd\mu N \quad (3-2-40)$$

From equation (3-2-37),(3-2-38)and(3-2-40):

$$F_2 = \frac{dW_{ch}}{dx} = \frac{-dV_{ch}}{dx} = n \frac{d\mu N}{dx} \quad (3-2-41)$$

Inserting equation (3-2-41) in (3-2-36) yields;

$$\frac{dE_0}{dx} = -n \frac{dW}{dx} - kT \frac{dn}{dx} + n \frac{d\mu N}{dx}$$

$$n(dE_0 + dW - d\mu N) = -kT dn$$

$$\frac{dn}{n} = \frac{-(dE_0 + dW - d\mu N)}{kT} \quad (3-2-42)$$

But;

$$d\mu N = \mu dN \quad dW = PdV$$

Thus equation (3-2-42) becomes;

$$\frac{dn}{n} = \frac{-(dE_0 + PdV - \mu dN)}{kT} \quad (3-2-43)$$

Integration of both side yields;

$$\int \frac{dn}{n} = -\frac{1}{kT} \int dE_0 - \frac{1}{kT} \int PdV + \frac{1}{kT} \int \mu dN$$

$$\ln n = -\frac{E_0}{kT} - \frac{1}{kT} \int PdV + \frac{\mu}{kT} \int dN + C_0$$

$$n = C e^{\frac{-(E_0 + \int PdV - \mu N)}{(kT)}} \quad (3-2-44)$$

But the internal energy U is related to the kinetic energy of individual particles. Therefore;

$$E_0 = \frac{1}{2}mv^2 = U$$

Hence;

$$n = Ce^{\frac{-U - \int PdV + \mu N}{kT}} \quad (3-2-45)$$

If P is constant, the number of particles is given by;

$$n = Ce^{\frac{-U - PV + \mu N}{kT}} \quad (3-2-46)$$

This e expression (3-2-44,46) resembles Gibbs statistical distribution law.

(3-2-6) Maxwell-Boltzmann Distribution for Average Thermal and Potential

The ordinary Maxwell-Boltzmann account for thermal as for as the total energy of the system is equated to the total thermal energy according to the relation;

$$\int En(E)dE = \frac{3}{2}NkT \quad (3-2-47)$$

The integral on the L.h.s is according to Maxwell distribution function equal to;

$$\int En(E)dE = \frac{3}{2}N\beta \quad (3-2-48)$$

The r.h.s of equation (3-2-47) account for thermal energy only. But it is well known that the bulk matter at rest in vacuum can have magnetic energy if it is a permanent magnet, although

the potential and kinetic energy of the bulk matter vanishes. If average magnetic potential is V , then the total energy of the system is equal to the thermal and magnetic energy, in this case equation (3-2-47) can be rewritten in the form;

$$\int En(E)dE = \frac{3}{2}NkT + \frac{3}{2}NV \quad (3-2-49)$$

Equation (3-2-48) and (3-2-49) yields;

$$\frac{3}{2}N\beta = \frac{3}{2}N(kT + V)$$

Thus;

$$\beta = kT + V \quad (3-2-50)$$

As a result the number of particles in cell is given by;

$$n_i = Ce^{-\beta E_i} = n = Ce^{\frac{-E_i}{(kT+V)}} \quad (3-2-51)$$

It is very interesting to note that this expression coincides with (3-2-12) which was obtained from plasma equation.

(3-3) Temperature Dependence of the Wavelength Spectrum of a Resonantly Pumped W-OPIC Laser

(3-3-1)Introduction

Optical pumping injection cavity (OPIC) lasers show great promise, exhibited higher temperature operation than electronically injected varieties. [46,47]

The placement of distributed Bragg reflector (DBR) mirrors on either side of the active region allows maximum absorption of photons by the quantum wells, resulting in increased efficiency [48,49]. Earlier approaches involved growing the sample such that the resonance corresponded to the available pump wavelength, an optical parametric oscillator (OPO) can tune the wavelength of the beam striking the sample. This becomes particularly significant as temperature is varied; the resonance wavelength shifts as temperature is increased, and the input beam wavelength must be tuned accordingly. Pumping at resonance both improves efficiency and reduces the threshold intensity for lasing behavior to begin [49].

By varying temperature, the characteristics of a mid-infrared OPIC laser can be better understood. Previous studies have shown a linear relationship between the emitted wavelength and temperature of a laser diode [48].

The distance between the peaks of the longitudinal modes can be used to determine how the index of refraction, n , of the laser varies using Equation (3-3-1)[50]. The change in n is given by

$$\Delta n = -n \frac{\Delta k}{k} + \frac{1}{2Lk} \quad (3-3-1)$$

Where k is the wave number, while L is the cavity length.

(3-3-2) Materials and Methods

(3-3-2-1) Experimental Setup

The OPIC laser studied was part of the ITV-1108 wafer grown by Sarnoff Corporation and used in T. C. McAlpine's thesis. This sample was grown via molecular beam epitaxy on a GaSb substrate. The W-well active region was topped with a strain balance layer of 40 Å AlSb. This was surrounded on each side by 100 Å hole-blocking layers made of

AlAs_{0.08}Sb_{0.92}. The top and bottom quarter wave stacks consisted of 10 and 18 periods, respectively, of 1451 Å GaSb and 1758 Å AlAs_{0.08}Sb_{0.92}. The third harmonic of a Spectra-Physics Quanta-Ray Pro-250 Nd: yttrium-aluminum-garnet (YAG) laser set to Q-Switch mode with 10 Hz frequency pumped a Spectra-Physics Quanta-Ray MOPO-PO (optical parametric oscillator.) The OPO allowed the wavelength with which the sample was pumped to be tuned, providing a means of pumping the sample at resonance. The sample was mounted in a cryostat and cooled to temperatures as low as 78 K using liquid nitrogen.

A polarizing cube of constant orientation was used in conjunction with a half wave plate to filter out a percentage of the signal; changing the half wave plate rotated the polarization of the input beam, allowing the polarizing cube to filter out a portion of the beam.

(3-3-2-2) Fourier Transformed Infrared Wavelength Spectra

The spectra were taken by a Varian FTIR Spectrometer, controlled with the Varian Resolutions-Pro software. The signal was received by a liquid-nitrogen-cooled HgCdTe detector. Step-scan nanosecond time-resolved spectroscopy (TRS) was selected as the scan mode. For each time step, a plot of response as a function of wave number was available. The signal reached the FTIR between 174.5 and 174.7 μs after the laser was triggered. To reach this time, 69 2.5 μs steps were taken, followed by 4 500 ns steps, providing rough spectra of the first 174.5 μs. To ensure sufficiently precise measurement of the signal of interest, 20 10 ns steps covered the range from 174.5 to 174.7 μs. The time-step at which this peak was maximized was saved and exported to Origin 7.5 software for analysis. The overall peak was fit with a Gaussian to find the center wave number (and as such wavelength) of this multi-mode peak. In cases with sufficient

resolution (0.25 cm⁻¹) each peak within the longitudinal structure was also fit with a Gaussian to determine its center. The difference between the peaks was calculated to allow determination of the change in index of refraction .

$$n_{\lambda}(T) = n_{\lambda}(300)e^{\alpha(T-300)} \quad (3-3-2)$$

The indices of refraction are dependent on the wavelength and temperature under consideration. Equation (3-3-2), provides a means of relating n for one wavelength at room temperature to another temperature. The constant α varies for different materials; for InAs and GaSb, $\alpha=9 \times 10^{-5} \text{ K}^{-1}$, and for AlSb and AlAs, $\alpha=5 \times 10^{-5} \text{ K}^{-1}$. Through this process, it became possible to determine Δn and begin analyzing the effect of optical.

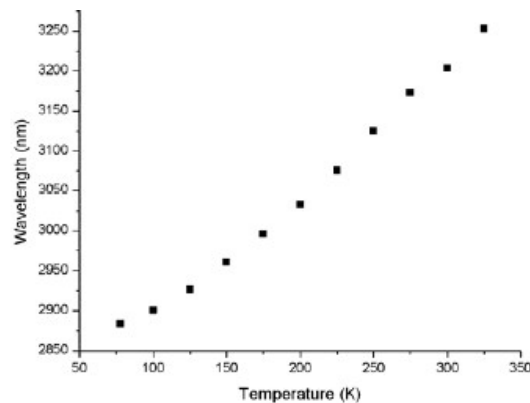


Fig (3-3-1): Temperature& Wavelength

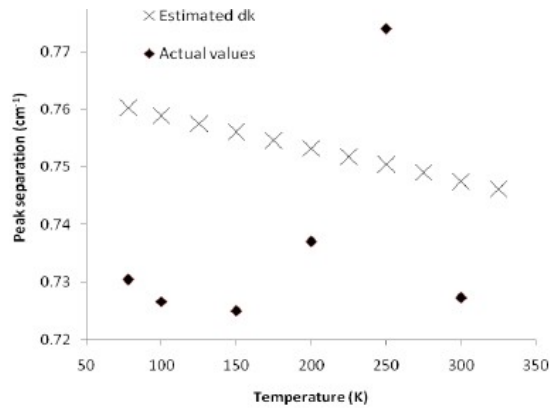


Fig (3-3-2): Temperature & Peaks

(3-3-3) Results

The emitted wavelength exhibited parabolic behavior with respect to temperature, as shown in Fig(3-3-1), increasing from 2.8 μm at 78 K to 3.3 μm at 325 K. The peak separations, Δk , are expected to decrease as temperature increases. To resolve the separations predicted by the estimates shown in Fig(3-3-2), a resolution of at least 0.35 cm^{-1} is necessary; thus, the 1 cm^{-1} data was taken with insufficient resolution and cannot be used to make an assertion about trends in Δn . More data at a sufficient resolution are necessary for a decisive relationship to be observed; however, preliminary data, shown in Fig. (3-3-2), with the correct resolution (0.25 cm^{-1}) shows peak separations on the same order of magnitude as those predicted.

(3-3-4) Discussion

The parabolic behavior of both resonant wavelength and emitted wavelength with respect to temperature does not agree with the expected

linear trend. one believe that an explanation for these discrepancies lies in Δn ; however, given the insufficient resolution used for the majority of the collected data, a definitive statement cannot be made about possible behaviors of Δn . In equation (3-3-2), knowing that α is used to describe a change in refractive index per degree Kelvin and the relationship being studied is the change in refractive index as a function of temperature, this level of agreement is encouraging. Currently, the only point representing more than a single spectrum is that for 78 K. ideally, after a greater number of spectra have been analyzed, a more definite trend will be observed.

The estimates of Δk shown in Fig(3-3-2), while on the same expected order of magnitude, do not follow the trend indicated by

$$\Delta k = \frac{1}{2nL} \quad (3-3-3)$$

This prediction assumes that $\Delta n=0$. However, the primary means of explaining the parabolic dependences of resonant and pump wavelengths on temperature appears to lie in a positive definite value of Δn . While the values of Δn are expected to be low enough to involve Δk values on the same order of magnitude as these estimates, the values themselves should be less than those shown in Fig (3-3-2) .

Finding accurate values for Δk and k from analyzing spectra will help us understand the gain dependence of Δn . Referring to the quantities listed in Equation(3-3-1), the cavity length and n vary linearly with temperature, while k varies parabolically with temperature. More data collection and analysis are required to determine the trend in Δk . While these values are known to change with temperature, n is a gain-dependent quantity, and optical pumping is known to increase gain by increasing the absorption of photons. This gain change leads to an additional change in Δn , as a greater portion of the pump beam must be allowed at higher temperatures to

continue measuring the laser output. Increasing the optical intensity also increases the heating that takes place as the sample receives the input beam. We aim to use the data to determine the overall shift in gain and the relative contribution of temperature-dependence, allowing better assessment of the gain-induced changes in lasing behavior.

(3-3-5) Conclusion

The emitted wavelength of a W-OPIC laser is a temperature-dependent quantity, increasing as temperature increases. This is in agreement with prior studies and calculated expectations. The relationship is parabolic, and by studying peak separations and analyzing n and Δn the cause of this parabolic relationship could be determined. The expected change in peak separation also exhibits temperature dependence. While our current data do not reflect the expected trend in Δk , the values are within .04 cm^{-1} of the prediction. The use of FTIR spectroscopy to analyze the signal emitted from an OPIC laser is a new technique in this lab, and this degree of accuracy bodes well for the continued analysis of these peak separations.

(3-4) Compensating Bragg Wavelength Drift Due to Temperature and Pressure by Applying an Artificial Strain

(3-4-1) Introduction

In today's fiber optic communication systems, fiber Bragg grating (FBG) are key components for wavelength division multiplexing (WDM) applications and dispersion compensation. FBG are short lengths of optical fibers that reflect a particular wavelength. They are made by laterally exposing the core of a single-mode fiber to a periodic pattern of intense ultraviolet light. The exposing produces a permanent increase in the refractive index of the fiber core creating a periodic index modulation

according to the exposure pattern. This fixed index modulation is called a grating.

The mathematical analysis is based on the assumption that the FBG has a uniform index modulation; its length is 2.5cm and the fiber core.[51]

Table (3-4-1) Constant Used in the Paper

Quantity	Symbol	Value
Bragg wavelength	λ_{B0}	1550 nm
Room temperature	T_o	25 °C
Thermo optical coefficient	α_n	$8.6 \times 10^{-6} \text{ } ^\circ\text{C}^{-1}$
Thermal expansion coefficient	α_Λ	$0.55 \times 10^{-6} \text{ } ^\circ\text{C}^{-1}$
Effective refractive index	n_{eff}	1.482
Grating period	Λ	0.5229 μm
Effective strain-optic constant	P_e	0.22

(3-4-2)The FBG Thermal Sensitivity

The Bragg grating resonance, which is the central wavelength of back-reflected light from a uniform Bragg grating, is given by[52]

$$\lambda_{B0} = 2 \Lambda n_{eff} \quad (3-4-1)$$

The shift in the Bragg grating central wavelength due to temperature changes is given by;

$$\Delta \lambda_{BT} = 2 \left[\frac{\partial n_{eff}}{\partial T} + \frac{\partial \Lambda}{\partial T} \right] \Delta T_{FBG} \quad (3-4-2)$$

$$\Delta \lambda_{BT} = \lambda_{B0} (\alpha_{\Lambda} + \alpha_n) \Delta T_{FBG} \quad (3-4-3)$$

α_{Λ} is the thermal expansion coefficient and α_n is the FBG thermo-optical coefficient.

The FBG thermal Sensitivity S_{FBG} is defined as

$$S_{FBG} = \frac{\Delta \lambda_{BT}}{\Delta T_{FBG}} \lambda_{B0} (\alpha_{\Lambda} + \alpha_n). \quad (3-4-4)$$

Hence, the Bragg central wavelength can be defined as[53]

$$\lambda_B = \lambda_{B0} + S_{FBG} \Delta T_{FBG} \quad (3-4-5)$$

Or

$$\lambda_B = \lambda_{B0} + \lambda_{BT} \quad (3-4-6)$$

Equation (3-4-6) is plotted in fig (3-4-1)

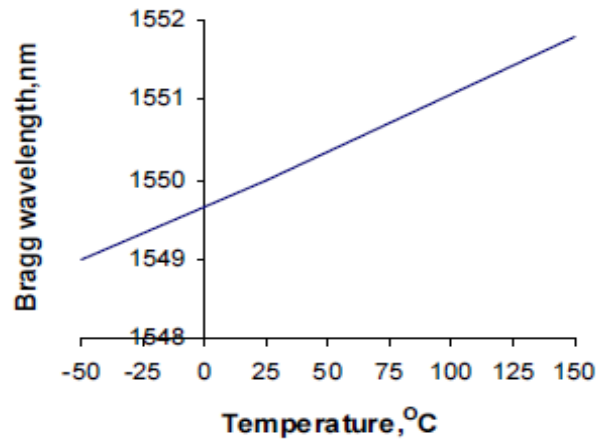


Fig (3-4-1) Bragg Wavelength, λ_B & Temperature

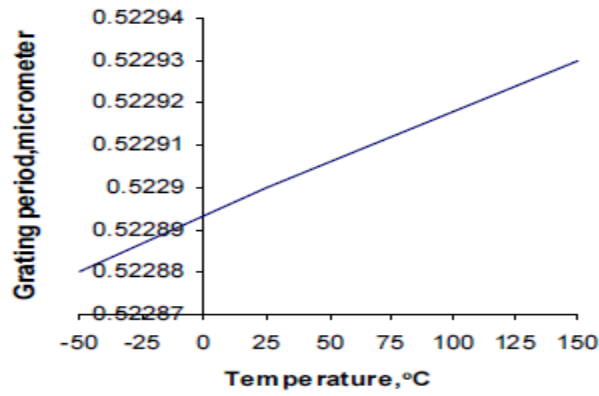


Fig (3-4-2) Grating Period & Temperature

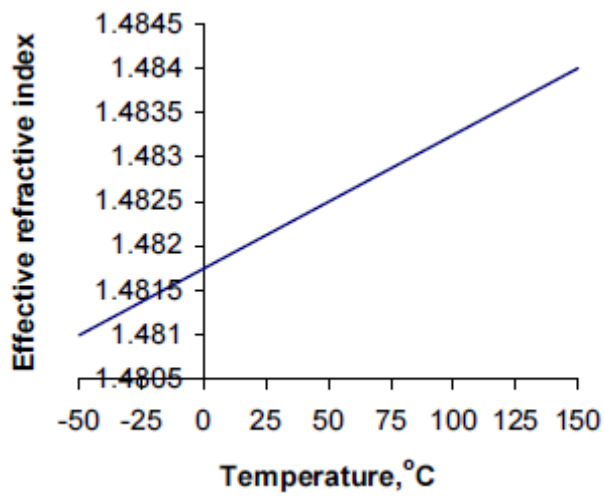


Fig (3-4-3) FBG Effective Refractive Index & Temperature

(3-5) Measurement of Temperature Using line-width Broadening

(3-5-1) Introduction

The spectrum of two oils, sesame and corn are displayed by the devices at different temperature.[54,55]

One uses Ultraviolet(UV) spectrophotometer model 6505 JENWAY company in the chemistry laboratory to study sample of corn oil and sesame oil to get the spectrum of these oils, the oils were mixed with ethanol. Since the heating of the samples causes evaporation, one cooling the samples to get different temperatures. [6](see figure(3-5-1)(3-5-2).

The sesam and the corn samples cooled for 4 or 5 different temperatures ,and their corresponding spectra are recorded by the ultra vilot spectrophotometer, the tables(3-5-1)(3-5-2)show the relation between temperature and spectral line-width of corn and sesame oils respectively.

Table (3-5-1): Relation Between Temperature θ & Spectral Line-width

$\theta \pm 1$	$\Delta\lambda \pm 10^{-9}m$
6	32
12	27
16	21
22	21
27	16

--	--

Table (3-5-2): Relation Between Temperature θ & Spectral Line-width

$\theta^{\circ} \pm 1$	$\Delta\lambda \pm 10^{-9}m$
10	30
14	25
18	20
27	20

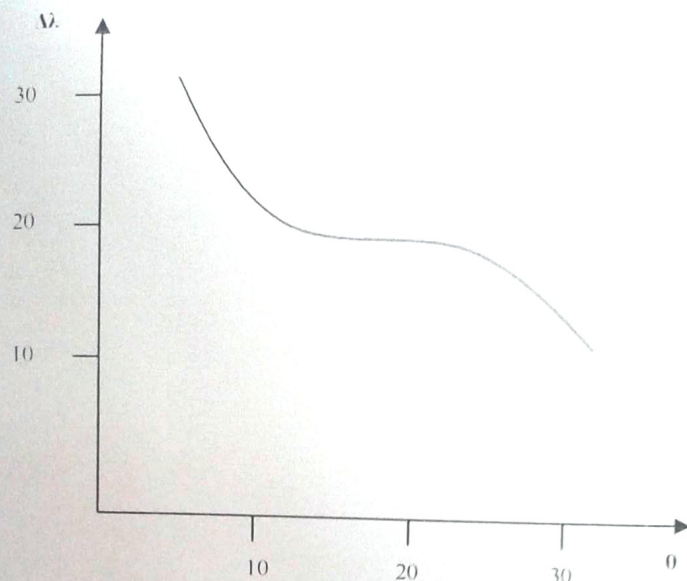


Figure (3- 5 - 1) : Relation Between Temperature θ° and Spectral Line-Width $\Delta\lambda$ for Corn

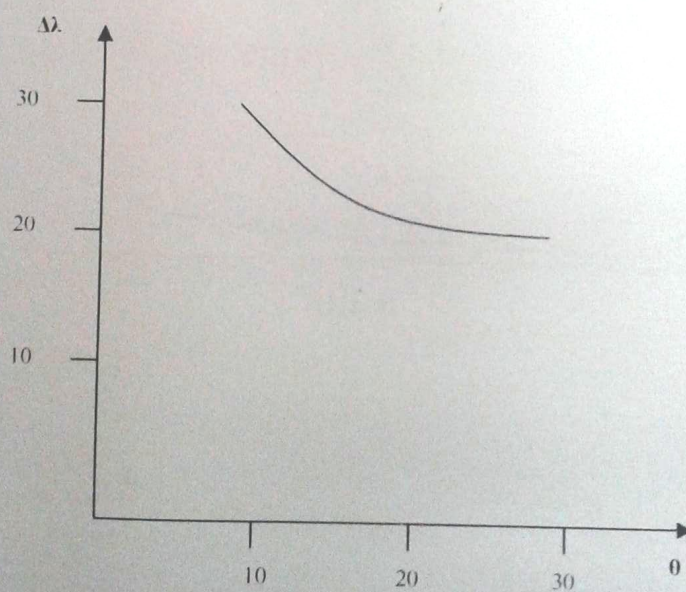


fig (3-5-2): Relation Between Temperature θ° and Spectral Line-Width $\Delta\lambda$ for Sesame

(3-5-2) Discussion

In view of tables (3-5-1) (3-5-2) and figures (3-5-1)(3-5-2) it's clear that the relation between temperature and broadening of the spectrum line is an inverse relation.

It is clear that $\Delta\lambda$ is inversely proportional to the relaxation time which in turn increases with temperature.

This is because as temperature increases the distance between atoms which increase in turn the relaxation time. Thus as temperature increases τ increases causing $\Delta\lambda$ to decrease.

Thus collision broadening dominates in this case. This is not surprising since oils are in a liquid state. For liquid state one expects that collision phenomenon dominate since the atoms are very close to each other. In this case atoms have no freedom to move freely and gain very high speed. Thus Doppler broadening does not dominate in this case. When one needs to utilize this technique to measure atmospheric temperature one expects no collision since atoms are far apart in a gases state. In this case can gain a high speed, thus Doppler broadening dominate in this case. As a result collision broadening as well as Doppler broadening can be used to measure temperature if a relation between τ_0 and temperature θ is obtained. Thus one can relate θ to $\Delta\lambda$ directly.

(3-6) Simultaneous Strain and Temperature Measurement Using a Superstructure Fiber Bragg Grating

(3-6-1) Introduction

Fiber Bragg gratings (FBG's) have generated much interest for use as sensors to measure strain, temperature, and other physical parameters. However, FBG's are sensitive to strain and temperature.[56]

(3-6-2) Principle

The SFBG is a special type of fiber Bragg grating fabricated using periodically modulated exposure over the length of a phase mask. As a periodically modulated FBG, the SFBG couples the forward-propagating LP mode to the reverse-propagating LP mode at a series of wavelength and introduces several narrow loss peaks in the transmission spectrum.

The SFBG also functions like a long-period grating (LPG) and couples the forward-propagating LP mode to forward-propagating cladding modes and introduces very broad-band loss peaks in the transmission spectrum. The wavelength shift of both the narrow-band and broad-band loss peaks are sensitive to strain and temperature, but with different responses. The relative wavelength shift of the broad-band loss peak with respect to the narrow-band peaks changes the intensity of the narrow-band loss peaks. Consequently, strain and temperature can be determined simultaneously from the wavelength and intensity of one of the narrow-band loss peaks in the transmission spectrum. Bhatia *et al.* have demonstrated that the slope of LPG's loss peaks is a logarithmic function of strain and temperature. It can be deduced that the transmitted intensity of an SFBG with the narrow-band loss peaks positioned on the slope of the loss peak is also a logarithmic function of strain and temperature.

Therefore, in addition to the shift in narrow-band loss peak wavelength, we now have a second parameter, the transmitted intensity, in decibels, vary linearly with strain and temperature.[57]

Therefore, strain change $\Delta\varepsilon$ and temperature change ΔT can be determined simultaneously by solving the following:[58]

$$\Delta I = A\Delta\varepsilon + B\Delta T \quad (3-6-1)$$

$$\Delta_{\lambda=C} = C\Delta\varepsilon + D\Delta T \quad (3-6-2)$$

Where ΔI is the change in the logarithm of the transmitted intensity and $\Delta_{\lambda=C}$ is wavelength shift of the narrow-band loss peak.

A (C) and B(D) are the respective strain and temperature coefficients of the loss peak's transmitted intensity (wavelength shift) of the SFBG, which can be determined experimentally by applying strain and temperature separately to the SFBG.[59]

(3-6-3) Experimental and Discussion

The SFBG was written in a “hydrogen-loaded” Alcatel dispersion-shifted single-mode fiber using a 10mm-long uniform phase mask, a 3-cm-long amplitude mask with a period of 500 μm , and an ArF excimer laser. During the writing process, the amplitude mask was placed on top of the phase mask. The 1-cm-long SFBG was then annealed at 160 °C for about 10 h to remove any unreacted hydrogen and unstable UV-induced defects. Fig. (3-6-1) shows the transmission spectrum of the SFBG after annealing. The spectrum was measured using a 1550-nm ELED source and an optical spectrum analyzer. Three narrow-band loss peaks are located at the slope of one of the broad-band loss peaks, which has a spectral width of 16 nm centered at 1568 nm. An expanded view of the transmission spectrum of the narrow-band peaks is also shown in the inset

of Fig. (3-6-1). The spectral width of these peaks is about 0.12 nm and centered at 1559.5, 1561.1, and 1562.7 nm. Any one of these peaks could be used to measure strain and temperature simultaneously. In this work, the 1561.1-nm peak was selected to demonstrate the sensing principle.

The experimental setup for determining the strain and temperature coefficients of the SFBG sensor is shown in Fig(3-6-2). The resolution of the OSA was set at 0.08 nm in all the measurements.

The SFBG was placed on top of a thermoelectric cooler (TEC) controlled with a TEC controller. The temperature coefficients and were measured by heating the sensor, with the TEC, under zero axial strain. The measured transmission spectrum of the SFBG with temperature varying from 20 °C to 95 °C with a step of 15 °C is also shown in Fig. (3-6-2). Fig. (3-6-3) shows that the transmitted power (in dBm) increases linearly with temperature in the range from 20 °C to about 110 °C. The broad-band spectrum shifts toward the longer wavelength at a faster rate than the narrow-band loss peaks. The wavelength shifts of the broad-band and narrow-band loss peaks with respect to temperature were measured to be 0.08 and 0.01 nm/ °C, respectively.

This explains the increase in transmitted power as temperature increases. A further increase in temperature shifts the narrow-band loss peak closer to a maximum (labeled as in Fig. (3-6-1)) of the spectrum, and thus the transmitted power no longer varied linearly with temperature. The values of and were estimated, using linear regression fits, as 0.0261 dB/°C ($R^2=.998$) and 11.3 pm/°C ($R^2=.9995$), respectively, over the range from 20 °C to 110 C. To measure the strain coefficients, strain was applied to the SFBG by fixing both ends of the grating with epoxy and stretched with a translation stage. The SFBG was maintained at 20°C with the TEC controller. The measured results are plotted in Fig. (3-6-4). The transmitted

power (in dBm) and wavelength shift vary linearly with strain over the range from 0 to 1200 $\mu\epsilon$. The values of A and C were estimated at -0.00148dB/ $\mu\epsilon$ ($R^2=.9958$) and 1.06 pm/ $\mu\epsilon$ ($R^2=.9996$), respectively. Inserting the values of these coefficients into (1) and (2), strain and temperature can be calculated from the wavelength and intensity of the narrow-band loss peak of the SFBG sensor. From Figs. (3-6-3) and (3-6-4), the accuracy of this particular sensor in measuring strain and temperature is estimated to be 20 in the range from 0 to 1200 $\mu\epsilon$ and $\pm 1.2^\circ\text{C}$ in the temperature range from 20°C to 110°C. The measurement range can be extended by using an SFBG sensor element with a broader LPG loss spectrum. It is interesting to note that the broad-band loss peak shifts toward the shorter wavelength whereas the narrow-band loss peaks shift toward the longer wavelength when the SFBG is stretched. This is because the strain coefficient of long-period grating fabricated in dispersion-shifted fiber is negative. The strain coefficients of the broad-band loss peaks and narrow-band loss peaks of the SFBG were measured to be -2.8 and 1.06 pm/ $\mu\epsilon$, respectively. Therefore, the narrow-band loss peaks move toward point M of Fig. (3-6-1) when the sensor experiences an increase in temperature but move toward point N of Fig. (3-6-1) when strain was applied to it. Consequently, the measurement range of strain and temperature can be extended at the expense of the other by positioning the narrow-band loss peaks closer to point M (to extent the strain measurement range) or point N (for temperature).

In conclusion, one reported the principle and experimental results of a novel SFBG sensor that allows simultaneously measurement of strain and

temperature. This sensor has the advantages of being simple and easy to fabricate. Since it is a transmissive-type sensor, neither expensive optical circulator nor lossy 3-dB coupler is needed for the sensing system. However, multiplexing of several sensor elements along a single fiber is not easy to implement due to the broad bandwidth of the loss spectrum of the LPG.

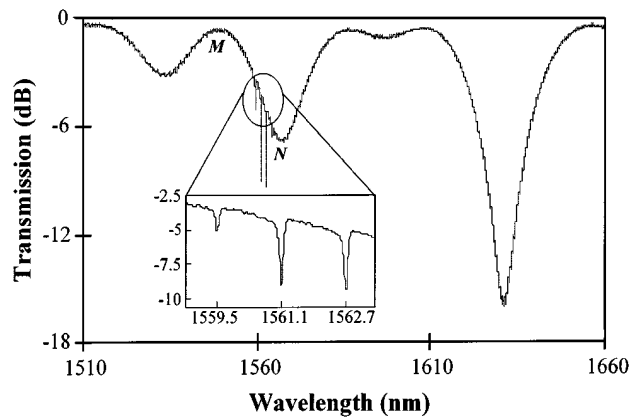


Fig (3-6-1): Transmission Spectrum of an SFBG.

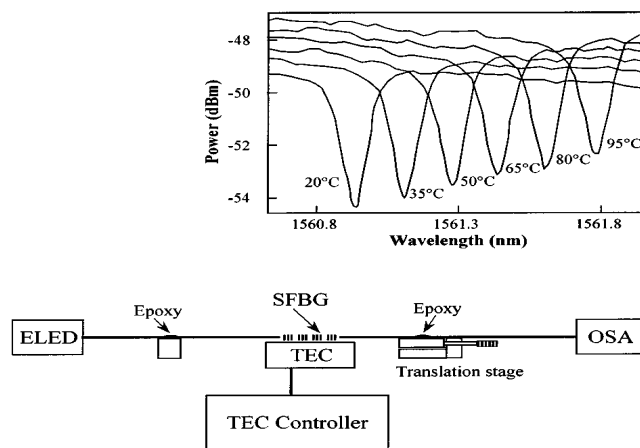


Fig (3-6-2): Experimental Setup for Determining the Strain and Temperature Coefficients

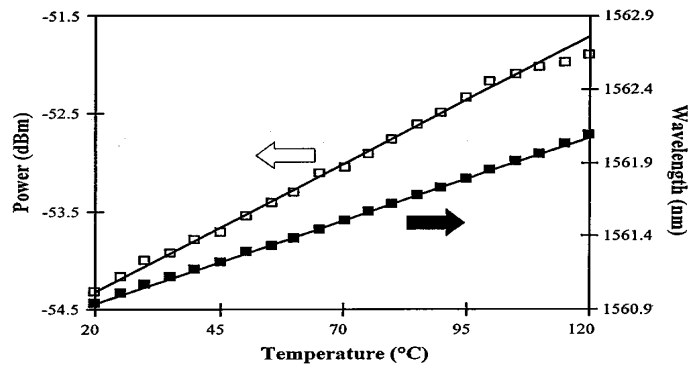


Fig (3-6-3): Relationship Between the Transmitted Intensity, Wavelength of the Loss Peak, and Temperature.

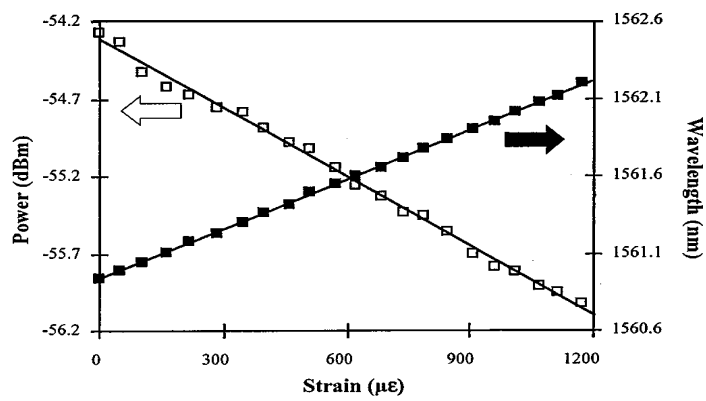


Fig (3-6-4): Relationship Between the Transmitted Intensity, Wavelength of the Loss Peak, and Strain.

Chapter Four

Relation between Temperature and Atomic Spectra Using Visible Light Spectral Techniques

(4-1)Introduction:

Temperatures affect atomic spectra through different mechanisms. To study this effect atoms of some gases are exposed to heat and their spectra at different Temperatures were studied

(4-2) Materials and methods:

The following Apparatus and Instruments are used in the experiment

(4-2-1)Apparatus and Instruments:

USB2000 Fiber Optic Spectrometer (Ocean Optics), Thermometer , Heater, Laptop, Source of [Helium Neon laser](#) -133, Power supply, , Connect cable, Origin program which specialist draw, analyze and address the different data and Test tubes (Borosilicate Glass)

(4-2-2) Gases:

Bhutan (C_4H_{10}), [Chlorine](#) (Cl_2), Carbon dioxide (CO_2), Carbon Monoxide (CO), [Fluorine](#) (F_2), Nitrogen (N_2), Neon (Ne) and Oxygen (O_2).

(4-2-3) USB2000 Spectrometer (Universal Serial Bus)

The USB2000 Spectrometer is connected to a notebook or desktop PC via USB port or serial port. When connected to the USB port of a PC, the USB2000 draws power from the host PC, eliminating the need for an external power supply.[60]



Fig (4-1) Ocean Optics USB2000 Fiber Optic Spectrometer

The USB2000 Spectrometer consists of the following components

1-SMA Connector

The SMA Connector secures the input fiber to the spectrometer. Light from the input fiber enters the optical bench through this connector.

2- Slit

The Slit is a dark piece of material containing a rectangular aperture, which is mounted directly behind the SMA Connector. The size of the aperture regulates the amount of light that enters the optical bench and controls spectral resolution.

You can also use the USB2000 without a Slit. In this configuration, the diameter of the fiber connected to the USB2000 determines the size of the entrance aperture.

3- Filter

The Filter is a device that restricts optical radiation to pre-determined wavelength regions. Light passes through the Filter before entering the optical bench.

4- Collimating Mirror

The Collimating Mirror focuses light entering the optical bench towards the Grating of the spectrometer.

Light enters the spectrometer, passes through the SMA Connector, Slit, and Filter, and then reflects off the Collimating Mirror onto the Grating.

5- Grating

The Grating diffracts light from the Collimating Mirror and directs the diffracted light onto the Focusing Mirror. Gratings are available in different groove densities.

6- Focusing Mirror

Focusing Mirror receives light reflected from the Grating and focuses the light onto the CCD Detector or L2 Detector Collection Lens.

7- L2 Detector Collection Lens

The L2 Detector Collection Lens (optional) attaches to the CCD Detector. It focuses light from a tall slit onto the shorter CCD Detector elements.

The L2 Detector Collection Lens should be used with large diameter slits or in applications with low light levels. It also improves efficiency by reducing the effects of stray light.

8- CCD (Charge Coupled Device) Detector (UV or VIS)

The CCD Detector collects the light received from the Focusing Mirror or L2 Detector Collection Lens and converts the optical signal to a digital signal.

Each pixel on the the CCD Detector responds to the wavelength of light that strikes it, creating a digital response. The spectrometer then transmits the digital signal to the OOIBase32 application.[60]

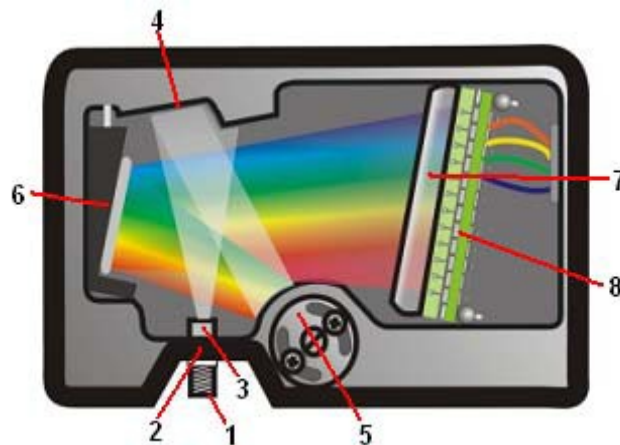


Fig (4-2)USB 2000 Spectrometer with Components

- 1- SMA Connector. 2- Slit. 3- Filter.
- 4- Collimating Mirror 5- Grating. 6- Focusing Mirror.
- 7- L2 Detector Collection Lens.
- 8- Charge Coupled Device (CCD) Detector.

(4-2-4) USB2000 Spectrometer Specifications[60]:

Dimensions:	89.1 mm x 63.3 mm x 34.4 mm
Weight:	190 g (without cable)
Power consumption:	90 mA @ 5 VDC
Detector range:	200-1100 nm
Detector:	2048-element linear silicon CCD array
Gratings:	14 gratings; UV through Shortwave NIR
Entrance aperture:	5, 10, 25, 50, 100 or 200 mm wide slits or fiber (no slit)
Order-sorting filters:	Installed long pass and band pass filters
Focal length:	f/4, 42 mm (input); 68 mm (output)
Optical resolution:	~0.3-10.0 nm FWHM (depending on grating and size of entrance aperture)
Dynamic range:	2 x 10 ⁸ (system); 2000:1 for a single scan
Stray light:	<0.05% at 600 nm; <0.10% at 435 nm; <0.10% at 250 nm
Sensitivity (estimate):	400 nm – 90 photons/count; 600 nm – 41 photons/count; 800 nm – 203 photons/count

Fiber optic connector:	SMA 905 to single-strand optical fiber (0.22 NA)
Data transfer rate:	Full scans into memory every 13 milliseconds
Integration time:	3 milliseconds to 65 seconds
Fiber optic connector:	SMA 905 to single-strand optical fiber (0.22 NA)
Operating systems:	Windows 98/Me/2000/XP when using the USB interface on a desktop or notebook PCs Any 32-bit Windows operating system when using the serial port on desktop or notebook PCs Windows CE 2.11 and above when using the serial port on palm-sized PCs

(4-3) Experiment Set Up

1- Glass tube is filled by gases.

2- Put the glass tube with gases on a heater to heat the gases.

3-Each gas should be heated in steps about one or two degrees. And the spectrum is recorded at each degree.

4-Use Thermometer to measure the temperatures of each gas, we put the thermometer into airtight glass tube.

5- The [Helium Neon laser](#)-633 beam is directed to incident on the glass tube.

6-Connecte the USB2000 Fiber Optic Spectrometer with Laptop the glass tube to be behind glass tube to receipt the beam transmitted through the glass tube.

7-Data were processed in the Origin program which analyze different data to find line width by(nm) , wavelength by(nm) , intensity and area at each temperature each gas.

8-The spectrum of each gas including the wavelength, intensity, band width and the area is recorded for each temperature.

9- Draw relations between intensity, wavelength of the spectrum line width of the transmitted radiation from each gas and temperature.

(4-4) Results

Table (4-4-1): Spectrum of Butane (C_4H_{10}) at Different Temperatures

T = temperature

λ = wavelength

I = Intensity

W=width

A = area

T(K)	λ (nm)	A(m²)	W (nm)	I(a.u)
300	630.73	4390.43	6.92	126.8
301	630.78	2536.69	6.96	125.89
303	630.83	2282.57	7.07	125.74
305	630.79	1645.95	7.03	125.79
307	630.78	1645.9	7.02	125.79
309	630.84	1855.9	7.16	125.13
311	630.78	1888.66	7.1	124.64

313	630	1698.66	7.03	124.79
315	630.83	1482.01	7.003	124.53
317	630.86	1560.78	7.03	123.96
318	630.84	1717.5	7.04	123.5
319	630.89	2037.01	7.08	123.46
320	630.95	1310.88	6.95	117.62
323	631.01	1265.28	7.02	116.95
324	631.01	1276.02	7.05	116.65

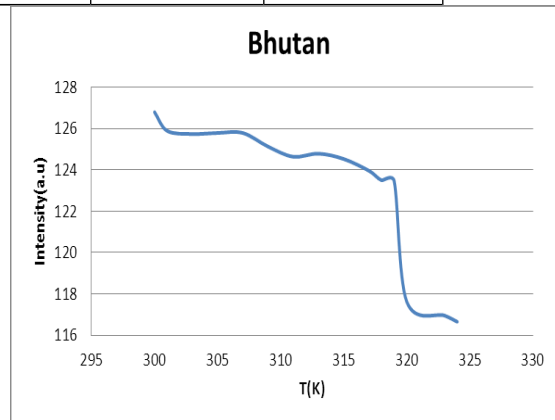
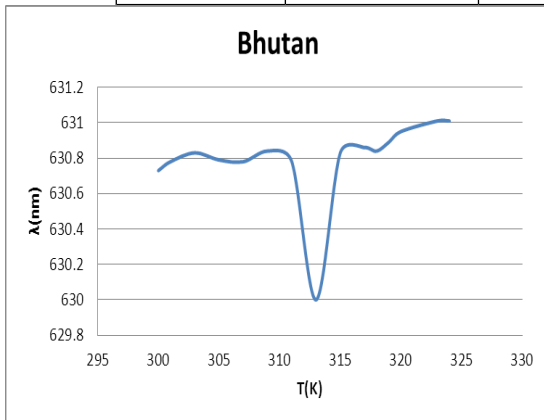
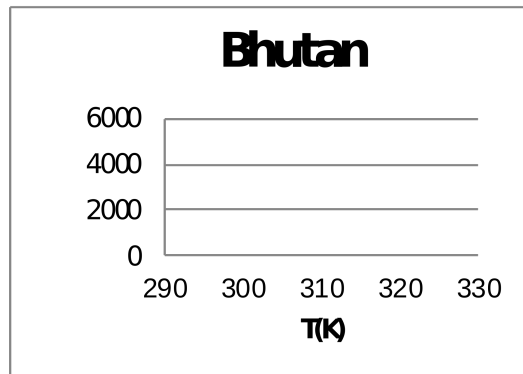
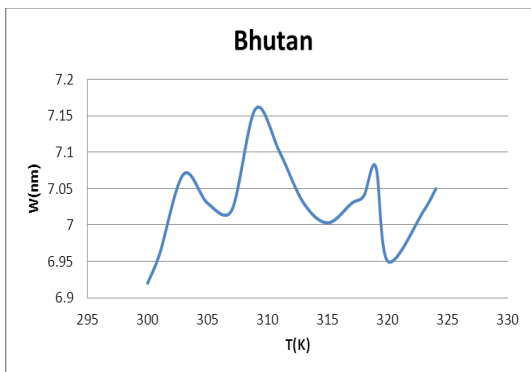


Fig (4-4-1-1) Relation Between Wavelength & Temperature

Fig (4-4-1-2) Relation Between Intensity & Temperature



Fig(4-4-1-3) Relationship Between Line width & Temperature

Fig (4-4-1-4) Relationship Between Area & Temperature

Table (4-4-2): Spectrum of Carbon Dioxide (CO₂) at Different Temperatures

T(K)	λ(nm)	A(m²)	W(nm)	I(a.u)
308	631.09	6721.97	7.09	104.78
310	630.69	3971.93	6.56	104.82
312	630.71	2990.83	6.61	104.98
314	630.68	2313.09	6.67	105.16
318	630.67	2672	6.59	105.105
319	630.73	2562.34	6.62	105.16
321	630.77	2788.17	6.63	104.95
323	630.75	2604.82	6.71	105.38
325	630.81	2746.3	6.76	105.25
327	630.75	2630.97	6.68	105.37
329	630.77	2896.99	6.58	105.56
331	630.66	3235.75	6.72	107.02
333	630.7	2852.53	6.67	109.16
336	630.64	2867.93	6.73	112.15

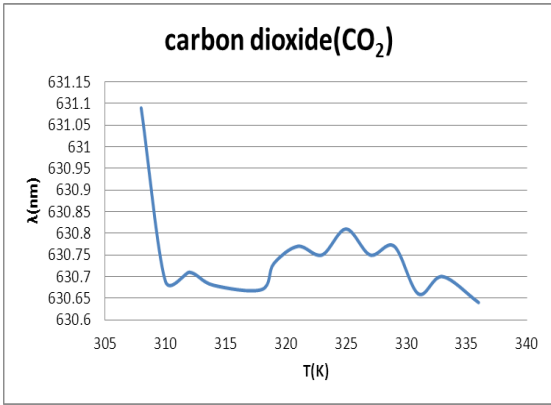
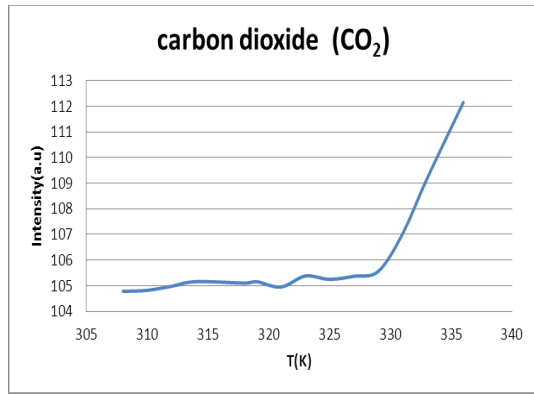
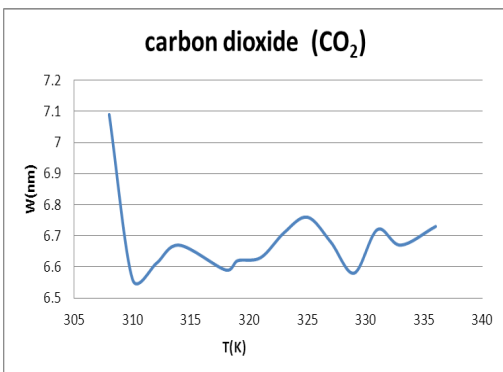


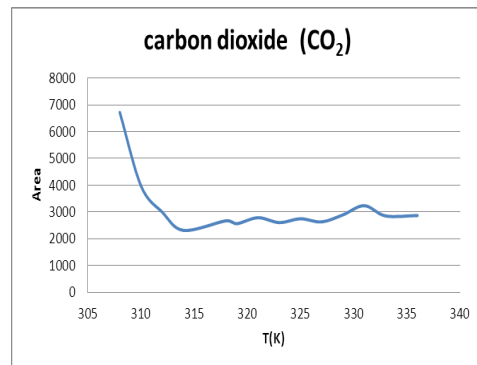
Fig (4-4-2-1) Relation Between Wavelength & Temperature



Fig(4-4-2-2) Relationship Between Intensity & Temperature



Fig(4-4-2-3) Relationship Between Line width & Temperature



Fig(4-4-2-4) Relationship Between Area & Temperature

Table (4-4-3): Spectrum of Carbon Monoxide (CO) at Different Temperatures

T(K)	λ (nm)	A(m²)	W(nm)	I(a.u)
305	630.81	7727.23	7.19	127.88
308	630.83	17902.95	7.52	128.35
310	631.15	23879.64	7.95	127.71
314	631.24	28752	8.02	127.72
316	630.95	35431.03	7.82	128.63
317	630.87	33455.02	7.63	129.07
318	630.97	35343.99	7.67	128.96
319	630.75	36682	7.59	128.89
320	630.5	31212.8	6.31	128.81
321	630.54	30925.51	6.29	129.12
323	630.53	35011.42	6.37	129.37
324	630.62	29236.35	6.28	132.05
325	630.62	30482.95	6.83	132.47
326	630.61	32561.45	6.4	134.94
328	630.6	28986.9	6.43	136.16

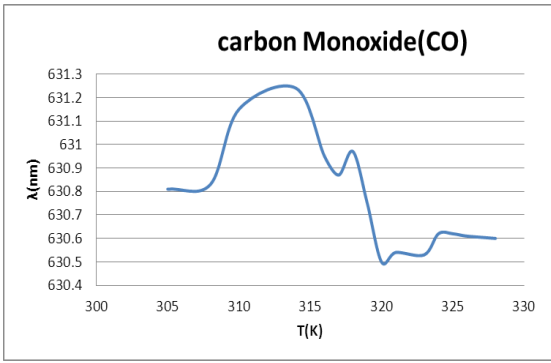
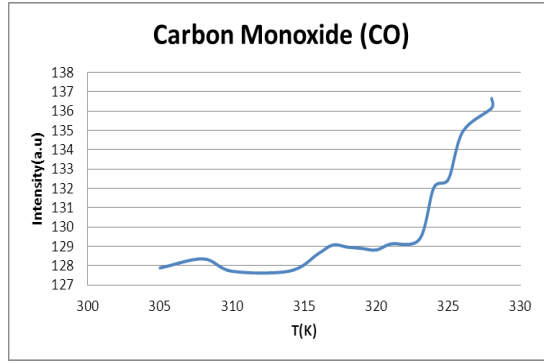
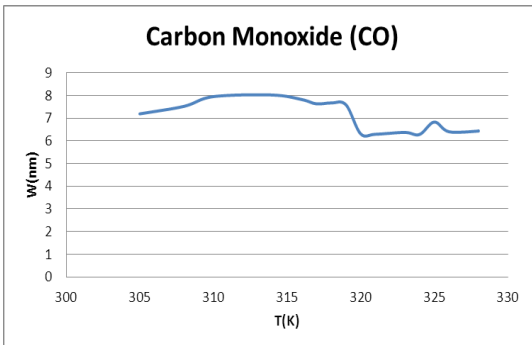


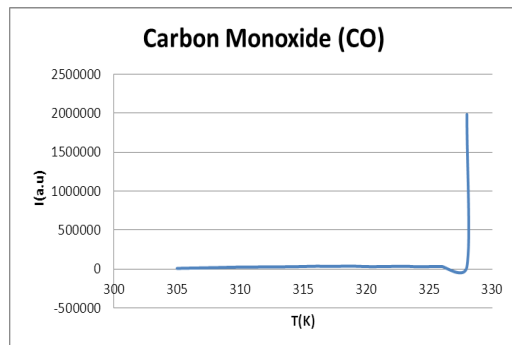
Fig (4-4-3-1) Relation Between Wavelength & Temperature



Fig(4-4-3-2) Relationship Between Intensity & Temperature



Fig(4-4-3-3) Relationship Between Line width & Temperature



Fig(4-4-3-4) Relationship Between Area & Temperature

Table (4-4-4): Spectrum of Oxygen (O₂) at Different Temperatures

T(K)	λ (nm)	A(m²)	W (nm)	I(a.u)
307	630.38	6.33	8357.87	121.82
309	630.39	6.45	8237.15	124.16
310	630.36	6.29	10776.64	105.39
312	630.39	6.34	9984.4	107.28
313	630.33	6.26	10333.1	108.35
317	630.36	6.36	10055.14	111.84
319	630.25	6.29	8871.58	114.79
320	630.1	6.37	10285.94	126.56
322	630.17	6.31	6953.2	126.2
323	630.14	6.37	7661.5	126.12

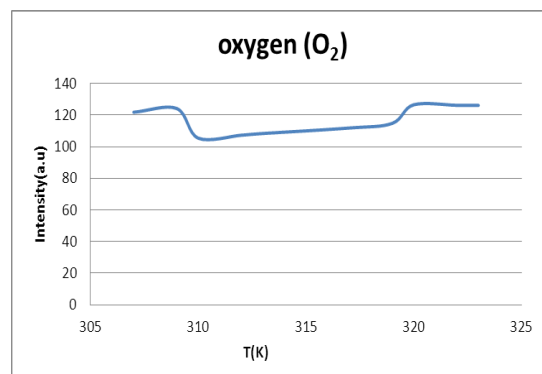
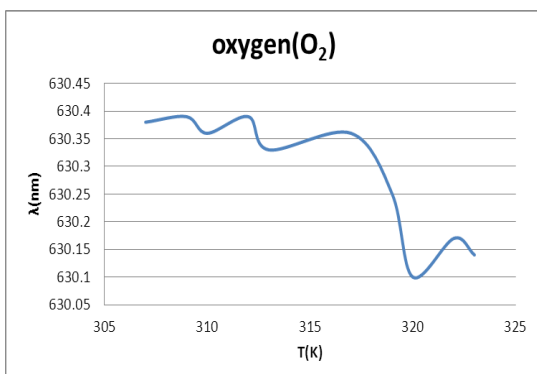
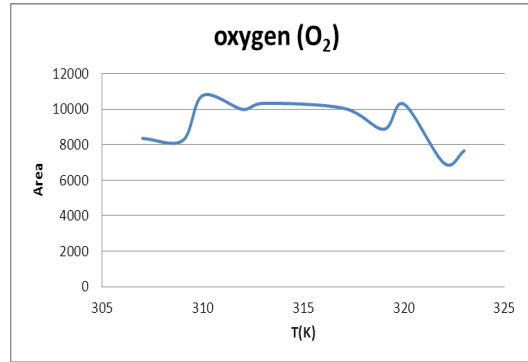
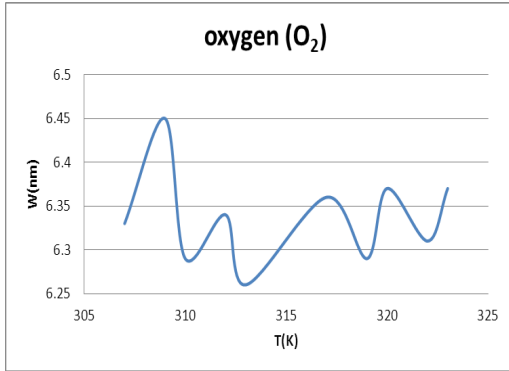


Fig (4-4-4-1) Relation Between Wavelength & Temperature

Fig(4-4-4-2) Relationship Between Intensity & Temperature



Fig(4-4-4-3) Relationship Between Line Width & Temperature

Fig(4-4-4-4) Relationship Between Area & Temperature

Table (4-4-5): Spectrum of Nitrogen (N₂) at Different Temperatures

T(K)	λ (nm)	A(m²)	W(nm)	I(a.u)
307	630.57	13210.75	6.46	106.37
308	631.05	22845	7	106.55

309	631.17	19689.5	7.03	105.14
313	631.14	26622.9	7.06	102.97
318	631.03	37660.7	7.02	101.47
323	631.04	22161.25	7.04	100.71
325	631.02	17831.8	6.99	100.73
326	631.15	20802.4	6.99	100.46
327	631.07	20115.56	7.05	100.21
328	631.05	23555.87	7.12	99.97
329	631.07	13968.94	6.99	101.27
331	631.1	13849.26	7.07	101.94
333	631.13	13601.3	7.07	102
334	631.15	14948.05	7.06	102.37
337	631.01	13328.25	7.02	103.29

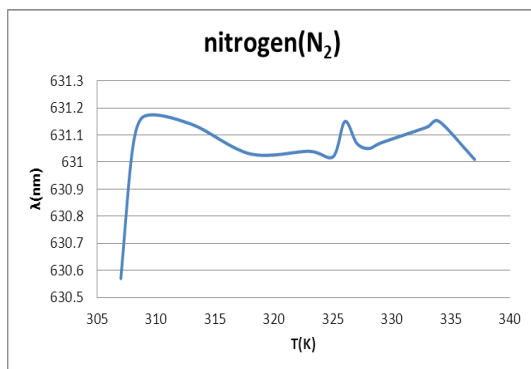
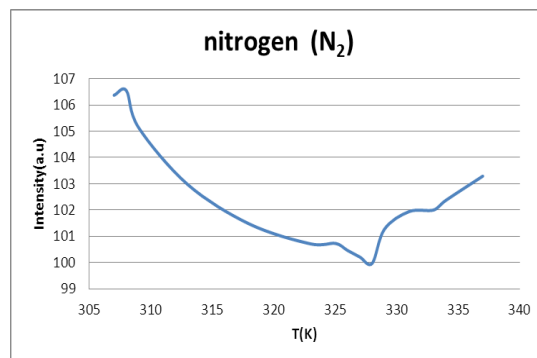


Fig (4-4-5-1) Relation Between Wavelength & Temperature



Fig(4-4-5-2) Relationship Between Intensity & Temperature

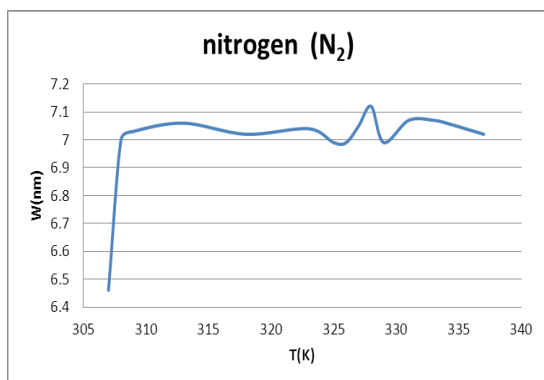
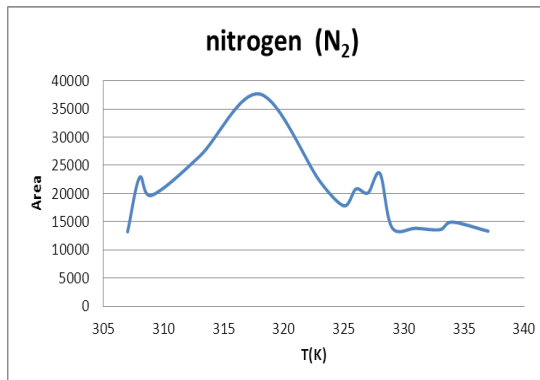


Fig (4-4-5-3) Relationship Between Line Width & Temperature



Fig(4-4-5-4) Relationship Between Area & Temperature

Table (4-4-6): Spectrum of Neon (Ne) at Different Temperatures

T(K)	λ (nm)	A(m²)	W(nm)	I(a.u)
307	630.66	6071.9	6.41	102.94
312	630.7	2287.59	6.48	103.25
313	630.76	1941.9	6.51	103.04
315	630.74	2111.14	6.46	103.45

317	630.73	3099.17	6.51	103.21
319	630.77	2276.22	6.53	103.26
320	630.78	3762.85	6.46	103.34
321	630.8	3515.7	6.51	103.39
322	630.77	2276.22	6.53	103.25
323	630.77	3179.53	6.48	103.4

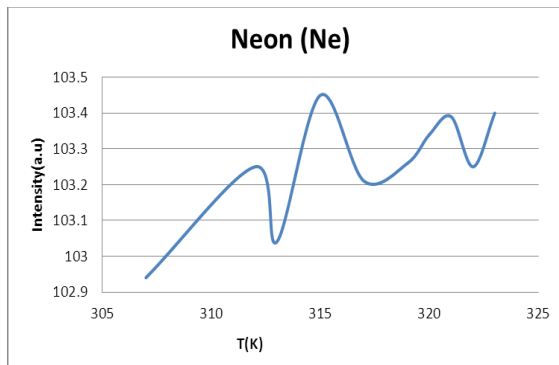
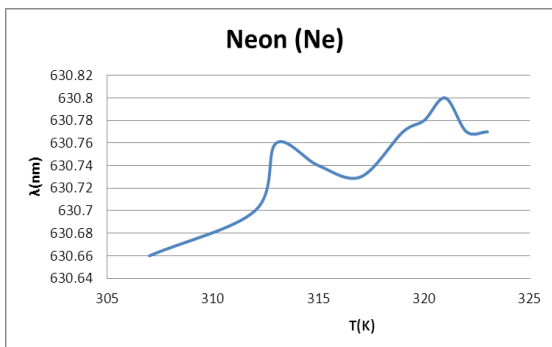
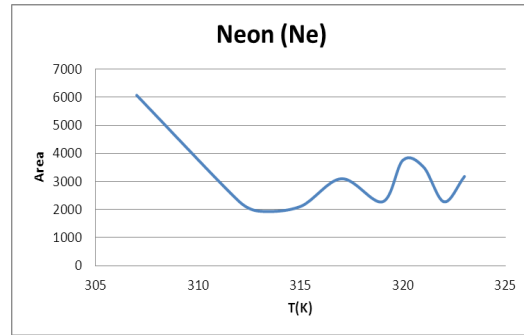
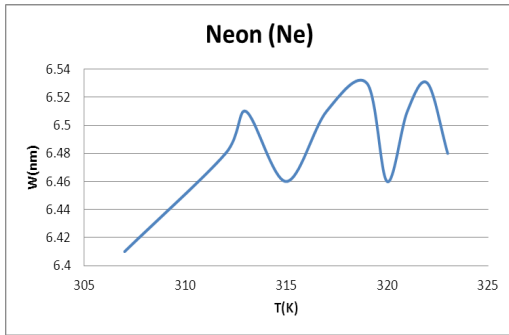


Fig (4-4-6-1) Relation Between Wavelength & Temperature Fig(4-4-6-2) Relationship Between Intensity & Temperature



Fig(4-4-6-3) Relationship Between Line Width & Temperature

Fig(4-4-6-4) Relationship Between Area & Temperature

Table (4-4-7): Spectrum of **Fluorine**(F₂)at Different Temperatures

T(K)	λ (nm)	A(m ²)	W(nm)	I(a.u)
304	631.02	6337.97	7.04	100.25
305	630.81	5964.04	6.44	98.63
307	630.9	5565.97	7.11	102.13
309	630.01	4442.99	7.16	102
311	631.01	5302.56	7.23	101.88
312	630.98	5332.11	7.25	101.52
314	631.06	4669.27	7.23	101.95

316	631.05	5193.09	7.16	101.82
317	631.08	5193.92	7.19	101.37
319	631.04	4549.7	7.2	101.66
321	631.11	3541.63	7.21	102.04
323	631.07	3351.55	7.13	102.3
325	631.08	4702.13	7.18	102.5

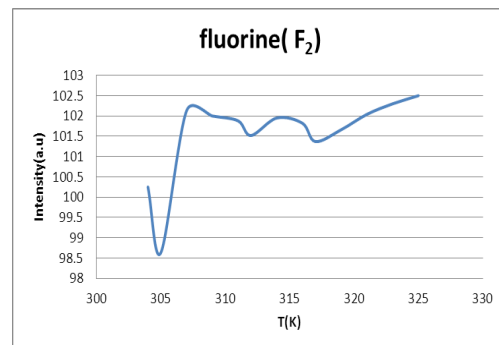
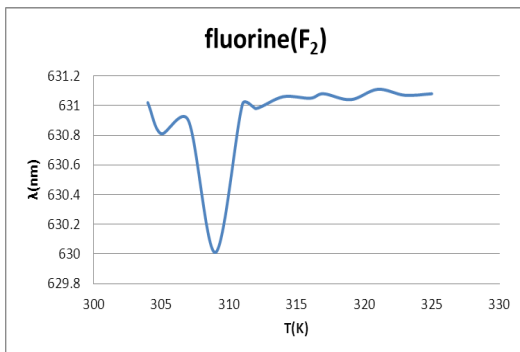


Fig (4-4-7-1) Relation Between Wavelength & Temperature Fig (4-4-7-2) Relationship Between Intensity & Temperature

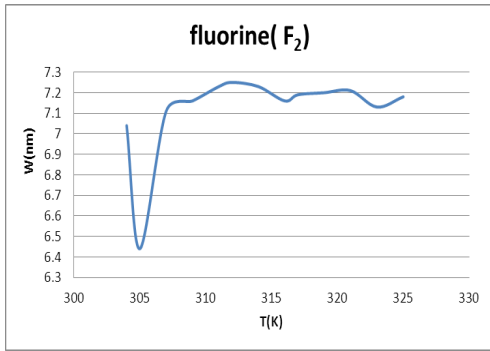


Fig (4-4-7-3) Relationship Between Line Width & Temperature

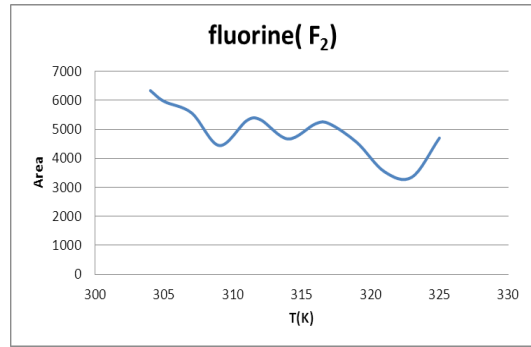


Fig (4-4-7-4) Relationship Between Area & Temperature

Table (4-4-8): Spectrum of [Chlorine](#) (CL₂) at Different Temperatures

T(K)	λ (nm)	A(m²)	W(nm)	I(a.u)
301	630.86	15934.5	6.92	122.23
303	630.83	7706.45	7.03	130.73
306	630.96	7478.8	7	124.24
308	630.95	8890.52	7.01	124.92
311	630.88	5738.32	7.08	126.31
313	630.94	5137.66	7.11	127.67
315	630.87	4995.6	7.01	127.81
317	630.88	4764.68	7.11	128.59
319	630.85	6501.06	7.006	129.27
321	630.93	4897.88	7.09	130.43
323	630.72	7777.74	6.88	131.22
325	630.77	6840.38	7.012	132.51
327	630.75	4907.18	6.92	134.15
329	630.75	5803.33	7.001	135.56
330	630.77	2866.74	7.05	137.006
331	630.83	2045.54	7.09	137.77

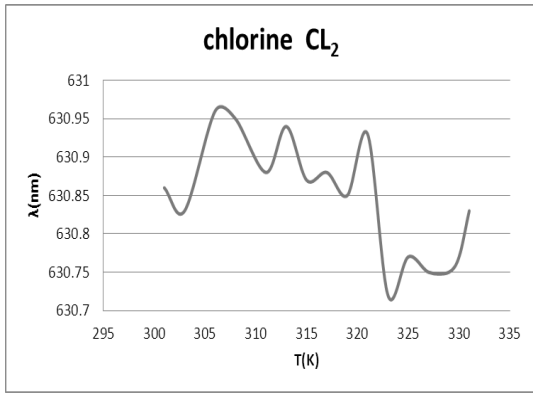
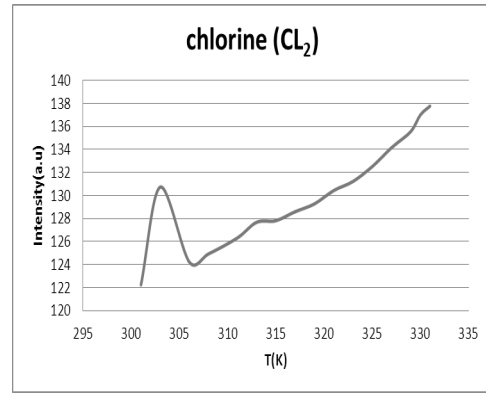
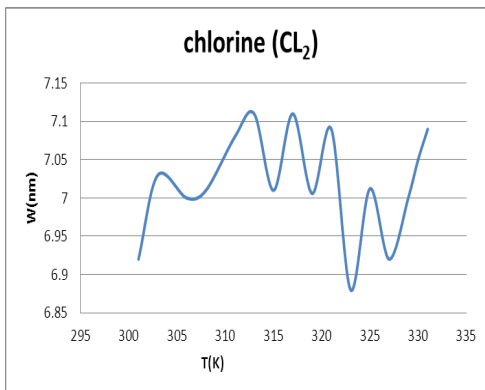


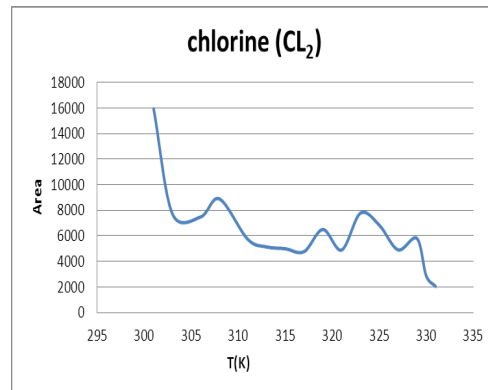
Fig (4-4-8-1) Relation Between Wavelength & Temperature



Fig(4-4-8-2) Relationship Between Intensity & Temperature



Fig(4-4-8-3) Relationship Between Line Width & Temperature



Fig(4-4-8-4) Relationship Between Area & Temperature

(4-5) Theoretical Interpretation

The behavior of gases can be explained by using statistical physics. This explanation is related to the fact. That gas consists of a large number of atoms and molecules. The electrons and atoms of gases can also be explained by using the laws of quantum mechanics. This is not surprising, since atomic and sub atomic microscopic particles are explained by using the laws of quantum mechanics.

(4-5-1) Thermal Equilibrium Statistical Interpretation

According to Maxwell distribution the density of particles is given by

$$n = n_0 e^{-\frac{E}{kT}} \quad (4-5-1)$$

It is quite natural to assume that the density of photons emitted n_p is proportional to the excited atoms or electrons density I. e

$$n_p = C_0 n = C_0 n_0 e^{-\frac{E}{kT}} \quad (4-5-2)$$

Where C_0 is a constant

Assume that the spectrum is formed due to the emission of free electrons surrounding the positive ion of the gas. In this case the potential is negative and attractive. By neglecting kinetic term, when the potential is very high in this case.

$$E = -V_0 \quad (4-5-3)$$

Therefore equation becomes (4-5-2)

$$n_p = C_0 n_0 e^{\frac{V_0}{KT}} \quad (4-5-4)$$

$$V_0 \sim \frac{9 \times 10^9 \times (1.6)^2 \times 10^{-38}}{r_0} \sim \frac{10^{-28}}{r_0}$$

$$\frac{V_0}{k} \sim \frac{10^{-5}}{r_0}$$

$$\text{For } r_0 \sim 10^{-5} m \quad \frac{V_0}{k} \sim 1 \quad (4-5-5)$$

The light intensity of the emitted photons is given by

$$I = C n_p = C C_0 n_0 e^{\frac{V_0}{KT}} = I_0 e^{\frac{V_0}{KT}} \quad (4-5-6)$$

By a suitable choice of (4-5-5) and using (4-5-6) parameters one can choose

$$I = I_0 e^{\frac{1}{T}} \quad (4-5-7)$$

$$I_0 = 10$$

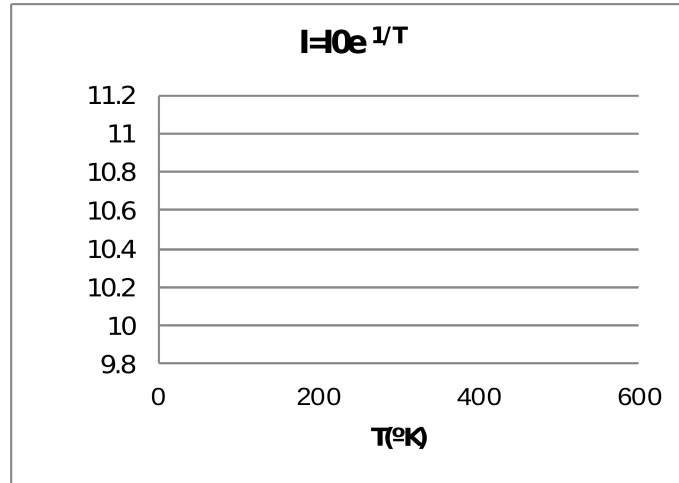


Fig (4-5-1)

(4-5-2) Non -Equilibrium Statistical System

The work done by Suhair Salih Makawy Suliman shows that for non-Equilibrium systems where the temperature, potential are no longer constant, but vary with position, the number density is given by

$$n = n_0 e^{-\frac{E}{\bar{E}}} \quad (4-5-8)$$

Where E stands for non-uniform varying energy, while \bar{E} represents the uniform energy. If one assumes that the electrons are affected by the bulk potential of positive ions, which is attractive, then

$$\bar{E} = -V_0 \quad (4-5-9)$$

$$E = kT \quad (4-5-10)$$

Substituting (4-5-9) and (4-5-10) in (4-5-8) yields

$$n = n_0 e^{\frac{KT}{V_0}} \quad (4-5-11)$$

In view of equations (4-5-2), (4-5-6) and (4-5-7) .The light intensity is given by

$$I = I_0 e^{\frac{KT}{V_0}} \quad (4-5-12)$$

Using (4-5-5)

$$\frac{V_0}{k} \sim 1$$

When

$$V_0 \sim k \sim 1 \times 10^{-22} \quad (4-5-13)$$

In this case equation (4-5-12) becomes

$$I = I_0 e^T \quad I_0 = 10 \quad (4-5-14)$$

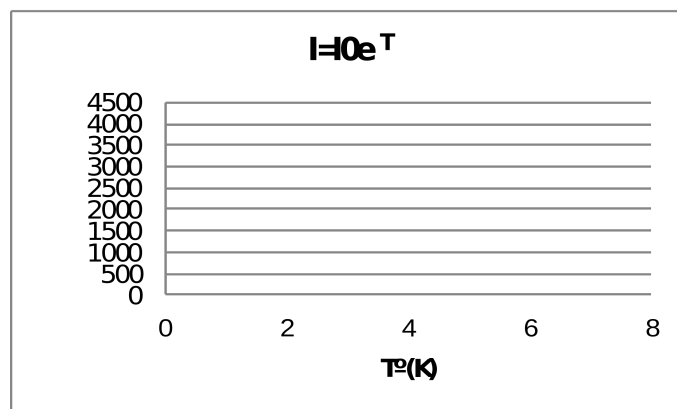


Fig (4-5-2)

When the electron energy is equal to thermal energy, beside energy V_r resulting from repulsive force

In this case

$$E = KT + V_r \quad (4-5-15)$$

If the back ground is the attractive uniform potential as in equation (4-5-2) then equation (4-5-11) becomes

$$n = n_0 e^{-\frac{V_r + KT}{V_0}} \quad (4-5-16)$$

Assuming that

$$\begin{aligned} V_r &\sim 100V_0 \\ V_0 &\sim 100k \sim 10^{-21} \end{aligned} \quad (4-5-17)$$

Using relations (4-5-2), (4-5-6), (4-5-16) and (4-5-17) yields

$$\begin{aligned} I &= I_0 e^{-\frac{V_r + KT}{V_0}} \\ I &= I_0 e^{100 + \frac{T}{100}} \end{aligned} \quad (4-5-18)$$

$$I_0 = 10$$

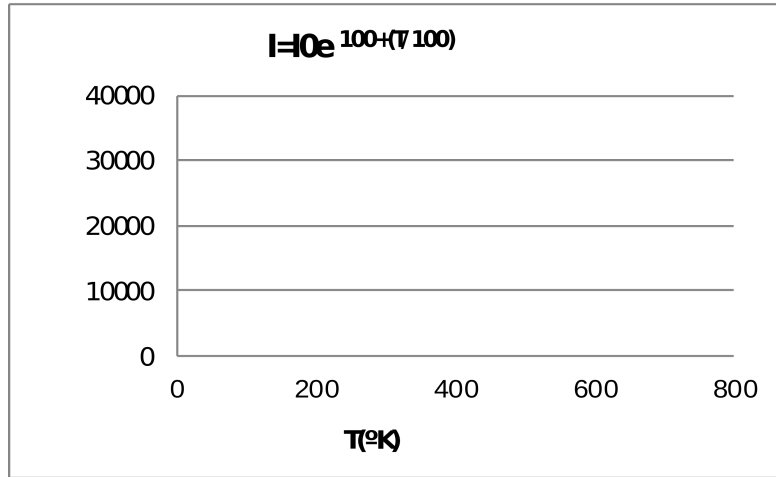


Fig (4-5-3)

If the energy resulting from the repulsive electron gas is assumed to be uniform, then

$$\bar{E} = V_r \quad (4-5-19)$$

When the electron energy is the thermal, beside the energy resulting from attractive ions V_0 then

$$E = KT - V_0 \quad (4-5-20)$$

In this case equation (4-5-8) reads

$$n = n_0 e^{\frac{V_0 - KT}{V_r}} = n_0 e^{\frac{V_0}{V_r} - \frac{KT}{V_r}} \quad (4-5-21)$$

In view of equations (4-5-2), (4-5-6) and (4-5-21), one gets

$$I = I_0 e^{\frac{V_0}{V_r} - \frac{KT}{V_r}} \quad (4-5-22)$$

Assuming

$$V_0 \sim 5V_r$$

$$V_r \sim k$$

(4-5-23)

One gets the light intensity in the form

$$I = I_0 e^{5-T}$$

(4-5-24)

$$I_0 = 2$$

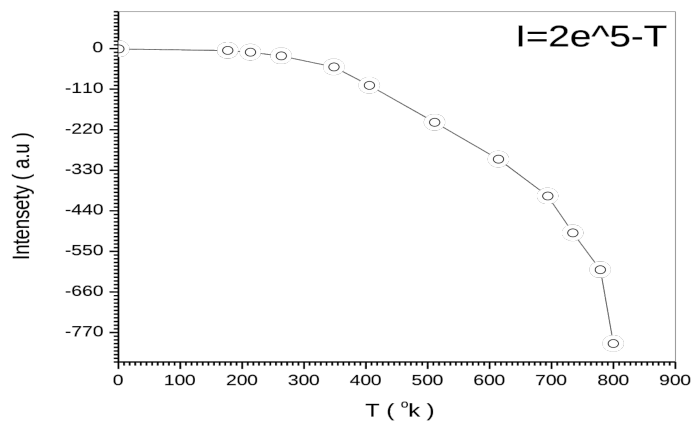


Fig (4-5-4)

One can assume gas where the thermal equilibrium

$$\bar{E} = KT$$

And assuming electron repulsive back ground

$$E = V_r$$

Thus equation (4-5-8) reads

$$n = n_0 e^{\frac{-V_r}{kT}} \quad (4-5-25)$$

For

$$V_r \sim k \quad (4-5-26)$$

Using also equations (4-5-2) and (4-5-6) one gets

$$I = I_0 e^{-\frac{1}{T}} \quad (4-5-27)$$

Set

$$I_0 = 10e$$

$$I = 10e e^{-\frac{1}{T}} = 10e^{1-\frac{1}{T}} \quad (4-5-28)$$

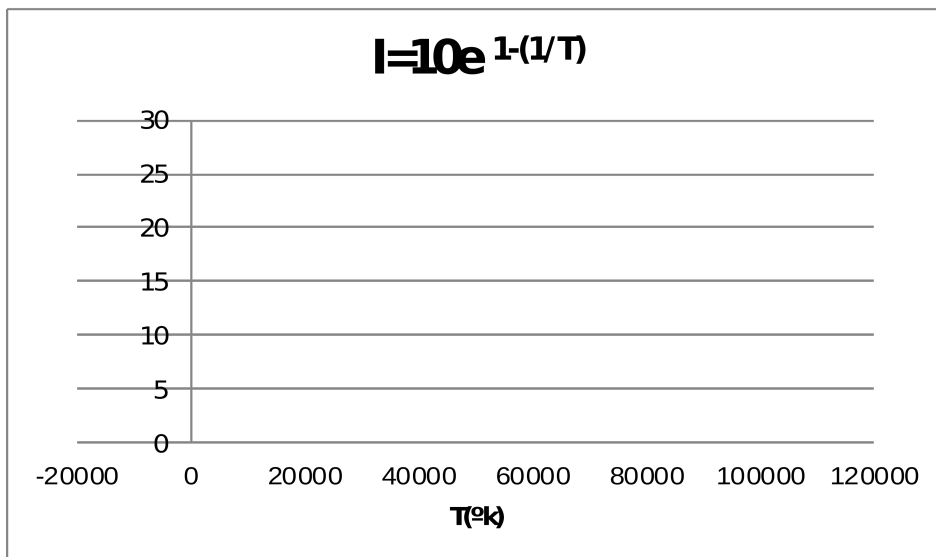


Fig (4-5-5)

(4-5-3)Complex Energy statistical Distribution

Heat energy results from collision of particles which lead to loss of energy that appears as heat thermal energy.

In some theories, like optical theorem the energy is written as summation of real and imaginary part. The real part stands for the particle energy, while the imaginary part represents the energy lost by the particle due to its interaction with the surrounding medium.

$$E = E_1 + iE_2 \quad (4-5-29)$$

If the uniform background is the attractive gas ions potential. Then

$$\bar{E} = -V_m \quad (4-5-30)$$

According to Shair .S model for non-equilibrium is given by system ,the distribution

$$n = n_0 e^{-\frac{E}{\bar{E}}}$$

Where E represents the non-uniform particle energy, where as \bar{E} stands for uniform particle energy

Thus substituting this in the equation

$$n = n_0 e^{-\frac{E_1 + iE_2}{V_m}}$$

$$n = n_0 e^{-\frac{E_1}{V_m}} e^{-\frac{iE_2}{V_m}}$$

$$n = n_0 e^{-\left(\frac{E_1}{V_m}\right)} \left[\cos \frac{E_2}{V_m} + i \sin \frac{E_2}{V_m} \right] \quad (4-5-31)$$

Considering the complex term standing for thermal energy

$$n = n_0 e^{\left(\frac{E_1}{V_m}\right)} \left[\sin \frac{E_2}{V_m} \right] \quad (4-5-32)$$

In view of equations (4-5-2), (4-5-6) and (4-5-32)

$$I = I_0 e^{\left(\frac{E_1}{V_m}\right)} \left[\sin \frac{E_2}{V_m} \right] \quad (4-5-33)$$

Assuming E_1 to be kinetic thermal energy of the particle and E_2 be the lost thermal energy such that

$$E_2 = C_0 E_1 = C_0 kT \quad (4-5-34)$$

$$V_m = k \quad (4-5-35)$$

It follows that

$$I = I_0 e^{T \sin C_0 T} \quad (4-5-36)$$

$$C_0 = \pi$$

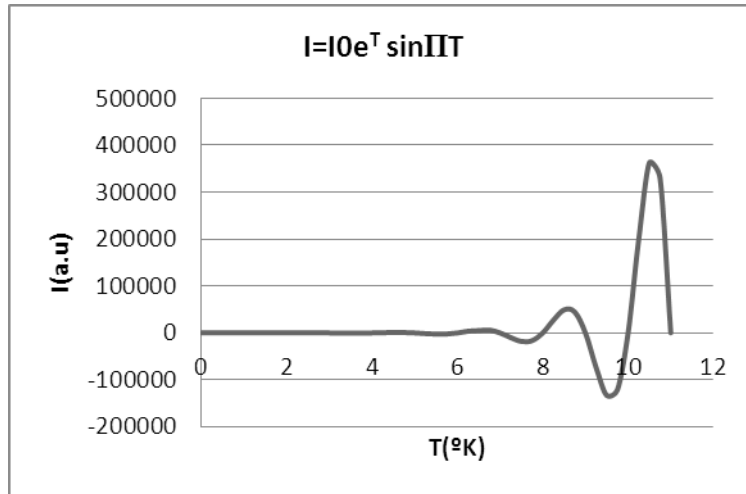


Fig (4-5-6)

However if the uniform background is the negative repulsive electron gas .In this case

$$\bar{E} = V_m \quad (4-5-37)$$

Thus equation (4-5-36) and (4-5-36) reduces to

$$n = n_0 e^{\left(\frac{-E_1}{V_m}\right)} \left[\cos \frac{E_2}{V_m} - i \sin \frac{E_2}{V_m} \right] \quad (4-5-38)$$

$$I = I_0 e^{\left(\frac{-E_1}{V_m}\right)} \left[\sin \frac{E_2}{V_m} \right] \quad (4-5-39)$$

In view of equations (4-5-36) and(4-5-35)

$$I = I_0 e^{-T} \sin C_0 T \quad (4-5-40)$$

$$C_0 = \pi$$

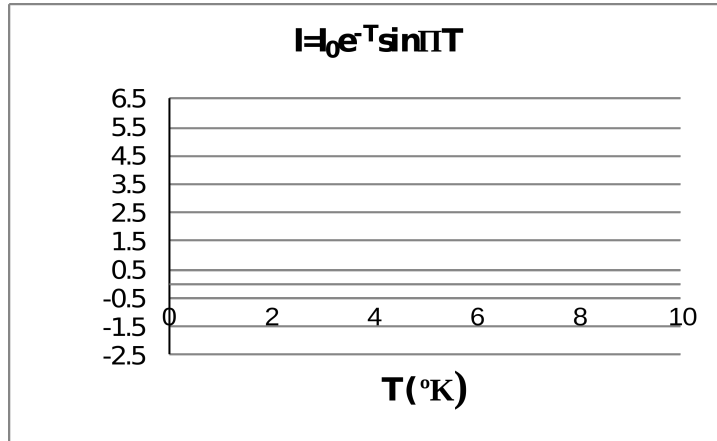


Fig (4-5-7)

(4-5-4) Statistical Interpretation

Using Maxwell Boltzmann distribution for electron

$$n_e = g e^{-\alpha} e^{-\beta(E_1 + iE_2)} \quad (4-5-41)$$

The imaginary part stands for absorption from medium or emission to the medium

$$E_e = E_1 + i E_2 \quad (4-5-42)$$

For photon the number of photons is given by

$$n_p = e^{-\beta(E_3 + iE_4)} \quad (4-5-43)$$

$$E_p = E_3 + i E_4$$

For composite system medium which consists of electrons emitting photons, the energy is given by

$$E = E_e + E_p \quad (4-5-44)$$

Where E is the energy of the electron in excited state, E_e is the electron energy in the ground state, while E_p is the photon energy. Thus the number of photon which is equal to the number of excited electrons is given by

$$n = e^{-\beta(E)} = e^{-\beta(E_e + E_p)} \quad (4-5-45)$$

For electron and photons colliding with particles medium, the energy lost appears as an imaginary part. Thus

$$n = e^{-\beta(E_1 + E_3)} e^{-j\beta(E_2)} e^{-j(\beta E_4)}$$

$$\text{For } E_1 \rightarrow 0 \quad E_3 \rightarrow 0$$

$$n = e^{-j\beta(E_2)} e^{-j(\beta E_4)} \quad (4-5-46)$$

$$= (\cos \beta E_2 - i \sin \beta E_2) (\cos \beta E_4 + i \sin \beta E_4) \quad (4-5-47)$$

Taking real part yields

$$n = \cos \beta E_2 \cos \beta E_4 \quad (4-5-48)$$

$$n = \cos \theta_2 \cos \theta_4 \quad (4-5-49)$$

$$I = \cos \theta_2 \cos \theta_4$$

If one assumes energy lost by the electron is 10 times that lost by the photon, it follows that

$$I = \cos 10\theta_4 \cos \theta_4 \quad \theta_2 = 10\theta_4$$

$$I = \cos 10T \cos T$$

$$T = 2, 4, 6, \dots$$

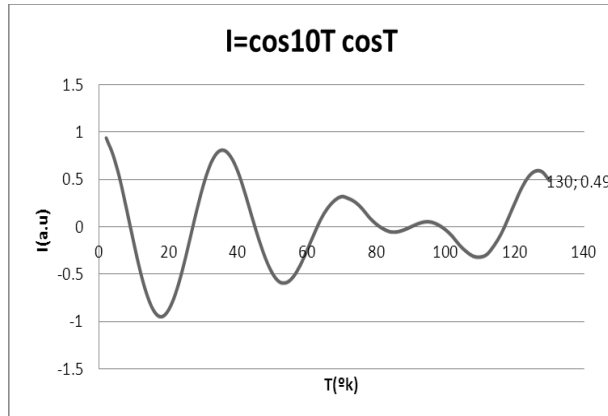


Fig (4-5-8)

(4-5-5) Quantum Mechanical Approach

According to the laws of quantum mechanics, the density and number of particles n are related to the wave function ψ

According to the relation

$$n = |\psi|^2 \quad (4-5-50)$$

But the intensities of radiation I is related to the total number of excited electrons per unit volume n

According to relations (4-5-2) and (4-5-6), where

$$I = C n_p = C_0 n \quad (4-5-51)$$

But the number of electrons n is given by

$n =$ number of atoms excited per second \times number of electrons excited per second

$$n = \frac{dn_a}{dt} \times \frac{dn_e}{dt} = \left(\frac{d|\Psi_a|^2}{dt} \right) \left(\frac{d|\Psi_e|^2}{dt} \right) \quad (4-5-52)$$

Now consider simple case of free particles. In this case such equation reads

$$-\frac{\hbar^2}{2m} \frac{\partial^2}{\partial x^2} \Psi = E\Psi \quad (4-5-53)$$

The solution will be

$$\Psi = A \sin \alpha x, \quad \Psi = -\alpha^2 \Psi \quad (4-5-54)$$

$$\frac{\hbar^2}{2m} \alpha^2 \Psi = E\Psi, \quad \alpha^2 = \frac{2mE}{\hbar^2} \quad (4-5-55)$$

The probability current density is given by equation to be

$$S = \frac{\hbar^2}{m} [\Psi^* \nabla \Psi] = A^2 \frac{\hbar^2}{m} [\alpha \sin \alpha x \cos \alpha x]$$

$$\frac{dm}{dt} = S = \frac{A^2 \alpha \hbar^2}{2m} \sin 2_{\alpha} x = c_0 \sin 2_{\alpha} x \quad (4-5-56)$$

But since

$$v = 0$$

$$E = \frac{mv^2}{2} = \frac{p^2}{2m}$$

$$2mE = p^2 = \hbar^2 k^2 \quad (4-5-57)$$

From (4-5-55)

$$\alpha^2 = k^2$$

$$\alpha = k = \frac{2\pi}{\lambda} = \frac{2\pi f}{\lambda f} = \frac{\omega}{v}$$

$$\alpha = \frac{\hbar\omega}{\hbar v} \quad (4-5-58)$$

If one heat particles are harmonic oscillator, thus according to equation (4-5-57) .The kinetic thermal energy becomes

$$KT = E = \hbar\omega \quad (4-5-59)$$

$$\alpha = \frac{KT}{\hbar v} \quad (4-5-60)$$

Thus for atoms and electrons see equation (4-5-56)

$$\frac{dn_a}{dt} = c_a \sin 2 \frac{KT}{\hbar v_a} x \quad (4-5-61)$$

$$\frac{dn_e}{dt} = c_e \sin 2 \frac{KT}{\hbar v_e} x \quad (4-5-62)$$

In view of equation (4-5-51) together with equations (4-5-2) and (4-5-6)

$$I = CC_0 n = CC_0 C_a C_e \sin 2 \frac{KTx}{\hbar v_a} \sin 2 \frac{KTx}{\hbar v_e} \quad (4-5-63)$$

at certain position x_0

$$I = C_a C_e \sin 2 \frac{KTx_0}{\hbar v_a} \sin 2 \frac{KTx_0}{\hbar v_e} \quad (4-5-64)$$

$$I = C_T \sin 2 \frac{KTx_0}{\hbar v_a} \sin 2 \frac{KTx_0}{\hbar v_e} \quad (4-5-65)$$

For Semiplicate let

$$20Kx_0 = \hbar v_0 \quad (4-5-66)$$

$$\frac{2Kx_0}{\hbar} = \frac{v_0}{10} \quad (4-5-67)$$

Thus

$$I = C_T \sin \frac{Tv_0}{10v_a} \sin \frac{Tv_0}{10v_e} \quad (4-5-68)$$

Let also
$$v_a = \frac{1}{10} v_e = \frac{1}{30} v_0$$

$$I = C_T \sin 3T \sin T = C_T \sin T \sin 3T \quad (4-5-69)$$

$$C_T = 10$$

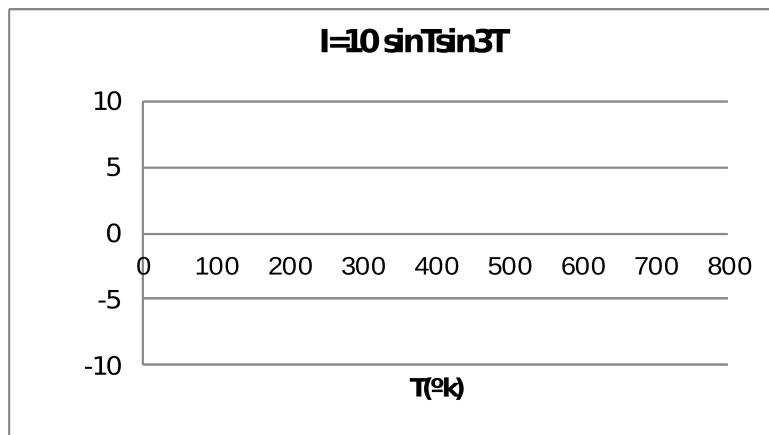


Fig (4-5-9)

Semi Classical Harmonic Oscillator Model(4-5-6)

Consider an electric field that causes oscillation of atoms and electrons to emit radiation. The equation of motion of the oscillating particle is given by

$$m a = -F \quad (4-5-70)$$

The force acting on the electron or atom is the electric field. Thus

$$F = E e \quad (4-5-71)$$

The displacement is given by

$$x_0 e^{-i\omega_0 t} = x$$

Hence, the speed and acceleration are given by

$$v = \dot{x} = -i\omega_0 x, a = \ddot{x} = -\omega_0^2 x \quad (4-5-72)$$

(Inserting (4-5-72) and (4-5-71) in (4-5-70)

$$\omega_0^2 x = -eE_m - \quad (4-5-73)$$

If resistive force for a medium of particles density n is the form

$$F_r = \frac{nmv}{\tau} = -\frac{nim}{\tau} \omega x \quad (4-5-74)$$

The frequency change from ω_0 to ω , thus the equation of motion becomes

$$ma = -eE - F_r \quad (4-5-75)$$

With

$$x = x_0 e^{-i\omega t}$$

$$v = \dot{x} = -i\omega x, a = \ddot{x} = -\omega^2 x \quad (4-5-76)$$

Therefore, inserting (4-5-73),(4-5-74) and(4-5-76) in(3-3-6)yields

$$-m \omega^2 x = -m\omega_0^2 x + \frac{inm\omega x}{\tau}$$

$$\omega_0^2 - \omega^2 = \frac{in\omega}{\tau}$$

$$(\omega + \omega_0)(\omega_0 - \omega) = \frac{in\omega}{\tau} \quad (4-5-77)$$

If

$$\omega \approx \omega_0, \omega + \omega_0 \approx 2\omega, \omega_0 - \omega = \Delta\omega \quad (4-5-78)$$

Thus

$$(2\omega) \left(\frac{\Delta\omega}{\tau} \right) = \frac{i n \omega}{\tau}$$

$$\left(\frac{\Delta\omega}{\tau} \right) = \frac{i n}{2\tau} \quad (4-5-79)$$

According to quantum harmonic oscillator model, if one treat the electrons and atoms as harmonic oscillators, their energy is given by

$$E_0 = \hbar\omega_0 \quad E = \hbar\omega \quad (4-5-80)$$

The energy difference due to friction is thus given by

$$\Delta E = E_0 - E = \hbar(\omega_0 - \omega) = \hbar\Delta\omega = \frac{i\hbar n}{2\tau} \quad (4-5-81)$$

The imaginary term is not surprising as far as the inelastic scattering is described by imaginary potential. This is known as optical theorem, in which inelastic scattering, where particles loose energy by collision, is described by a complex potential.

In atomic spectra thus thermal energy leads to lost or gain of energy by collision leading numerically to the change of frequency in the form

$$\Delta f = \frac{\Delta\omega}{2\pi} = \frac{n}{4\pi\tau} \quad (4-5-82)$$

The coresponding change of length takes the form

$$\begin{aligned} f_0 - f &= \frac{c}{\lambda_0} - \frac{c}{\lambda} = \frac{c(\lambda - \lambda_0)}{\lambda\lambda_0} = \Delta f \\ &= \frac{c\Delta\lambda}{\lambda^2} = \frac{c^2}{c\lambda^2} \Delta\lambda = \frac{f^2}{c} \Delta\lambda \end{aligned} \quad (4-5-83)$$

where

$$\lambda \approx \lambda_0 \quad \Delta\lambda = \lambda - \lambda_0 \quad (4-5-84)$$

Thus, in view of (3-3-15), equation (3-3-13) gives

$$\Delta\lambda = \frac{nc}{4\pi f^2 \tau} = \frac{\pi nc}{\omega^2 \tau} \quad (4-5-85)$$

But since the number density is related to the wave function according to the relation

$$n = |\Psi|^2$$

Thus

$$\Delta\lambda = \frac{\pi c |\Psi|^2}{\omega^2 \tau} \quad (4-5-86)$$

Using the complex energy statistical distribution in equation

$$n = n_0 e^{E_1/V_m} \sin \frac{E_2}{V_m} \quad (4-5-87)$$

Following the same procedures in equation from (4-5-34) to (4-5-40) one gets the line width in the form

$$w \sim \Delta\lambda \sim e^{-T} \sin \pi T \quad (3-3-88)$$

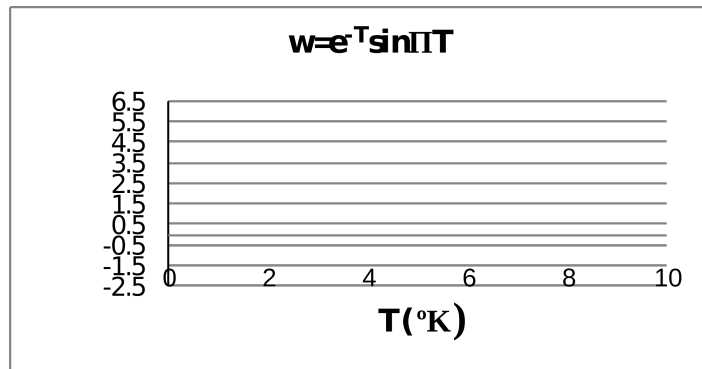
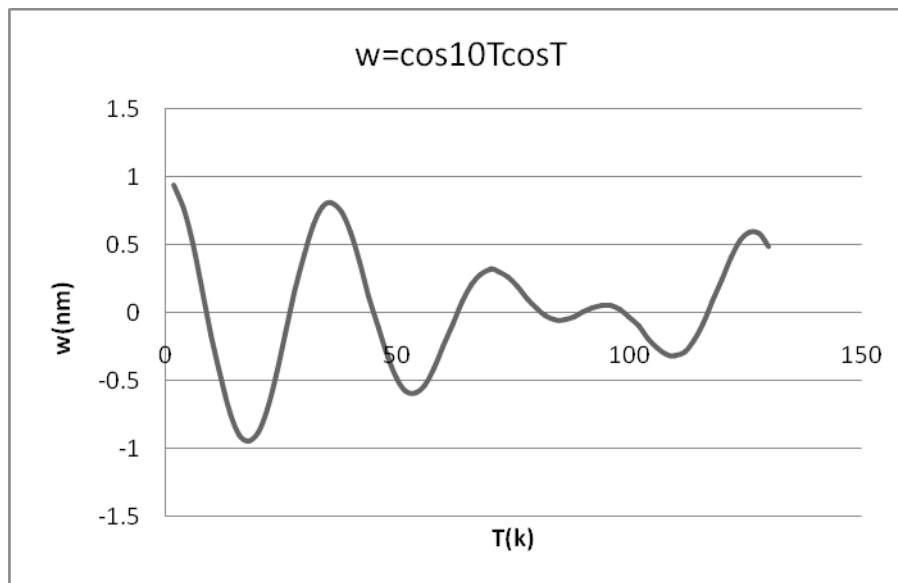


Fig (4-5-10)

If one using the expression for the total number of electrons resulting from multiplying the number of electrons in each atom by the number of atoms, one gets

$$w \sim \Delta\lambda \sim \cos\beta E_2 \cos\beta E_4$$

$$\sim \cos 10T \cos T \quad (4-5-89)$$



(Fig (4-5-11

Where one follows the same procedures used for the intensity expression derived for complex energy by using Maxwell's distribution.(see equation 4-5-69)

The use of quantum expression in equations (4-5-69) together with equation (4-5-69) leads to

$$w \sim \Delta\lambda \sim \sin T \sin 3T \quad (4-5-90)$$

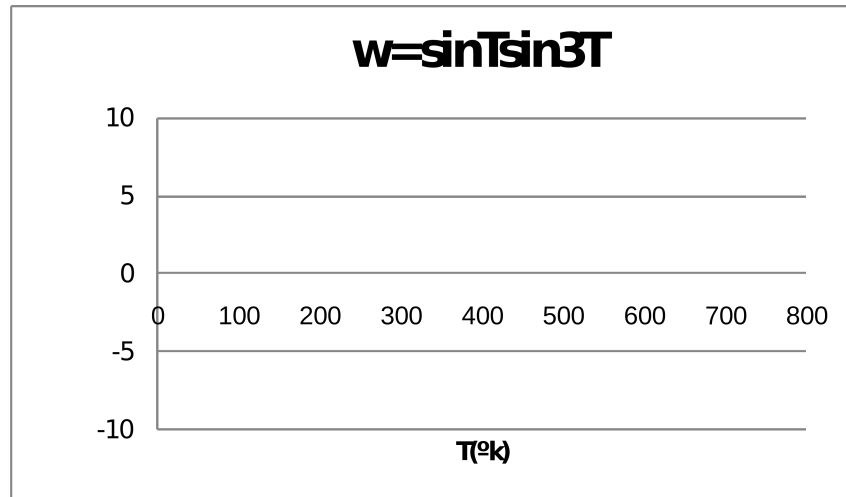


(Fig (4-5-12

(Discussion 7-4(

Fig (4-4-1-2) shows the relation between Intensity and temperature for Bhutan (${}^4_4H_{10}$),the curve of this relation resembles that of fig (4-5-4).This means the Bhutan gas the homogenous repulsive electron gas potential is almost constant compared to attractive ion potential and temperature.

Fig (4-4-2-2) shows the relation between intensity and temperature for Carbon dioxide (CO_2) which has a curve that resembles the curve in figs (4-5-2) and (4-5-3) .This indicates that the attractive positive ions looks homogeneous and stable compared to temperature. This is not surprising since the gas was heated at the bottom by a heater. This means that the bottom is hotter than the top part of the gas .Thus the temperature is not uniformities.

In Fig (4-4-3-2) the relation between Intensity and temperature for Carbon Monoxide (CO) which is displayed in this fig, resembles the curve of figs (4-5-2) and (4-5-3). This is not surprising, since for both figures the

statistical distribution is based on the homogeneity of the ionic field and non-homogeneity of temperature. The non-homogeneity of temperature results again from the fact that the bottom of the gas exposed to a heater is very hot compared to the top of the gas.

However Fig (4-4-4-2) shows that the relation between Intensity and temperature for Oxygen (O₂) can be easily explained by fig (4-5-5) where the repulsive homogeneous electron field dominates, compared the attractive ionic field. Fig (4-4-5-2) shows for Nitrogen (N₂) its spectrum is displayed by the relation between Intensity and temperature. The curve of this relation resembles fig (4-5-1) which shows homogeneity of temperature compared to less homogeneous attractive crystal field. The relation between Intensity and temperature for Neon (Ne) see fig (4-4-6-2) resembles that obtained theoretically in equations (4-5-32) and (4-5-36), for the case when the temperature is non-uniform [see fig (4-5-6)]. Thus

$$E_1, E_2 \sim kT$$

And the electric static potential is assumed to be uniform. This agrees with the fact that the gas is heated at the bottom, where it is very hot, while its temperature at the top is less. The same empirical relation for Ne can be explained by using quantum mechanics model in Fig (4-5-9) .

Fig (4-4-7-2) shows the Relation between Intensity and temperature for [Fluorine](#) (F₂) the curve of this relation resembles that of fig (4-5-7). This means the homogeneity of the repulsive electron gas .

However Fig (4-4-8-2) shows that the Relation between Intensity and temperature for [Chlorine](#) (Cl₂) can be explained by fig(4-5-7) . This indicates that the homogeneous repulsive electron gas.

The model based on semi classical harmonic oscillator and quantum mechanics explains the effect of temperatures on the line width of the

spectrum for the gases Butane (C_4H_{10}), Neon (Ne), [Fluorine](#) (F_2) and [chlorine](#) (Cl_2).

The comparison of Figs (4-4-1-3), (4-4-6-3), and (4-4-8-3) with Fig , (4-5-12) and (4-5-11) and(4-4-7-3) with(4-5-10). shows that the theoretical relations of line width with temperatures resembles the corresponding empirical relation.

(Conclusion:-4 (7

The effect of temperature on spectra of gases can be explained by using non equilibrium statistical laws derived from plasma equation as well as a quantum and semi classical models for harmonic oscillator..

The promotion of these models in the future may successfully be applied to determine the atmospheric temperatures at different layers.

(4-8)Recommendation

- 1-The temperature range for future study must be widened by cooling .
- 2-more gases should be examined to relate temperature to spectrum
- 3-New techniques that relate temperature to light wave length and spectrum area is needed.

References

- [1] Cooney, Measurements of atmospheric temperature profiles by Raman back scatter, 1972.
- [2] M.Endemann and R.L.Byer Remote sensing Measurements of atmospheric temperature and humidity (at $1.77\mu\text{m}$, 1980).
- [3] N. Matura, Y.masuda, H.Lnuki, S.kato, S.fukao, T.sato and T Tsuda Radio Acoustic measurements of temperature profile in the Troposphere and stratosphere, (Macmillan, 1986.)
- [4] A .Beiser, Concept of Modern Physics,(Mc Hill, New York, 1990).
- [5] J. R. Meyer, et al. "Type-II quantum well lasers for the mid wavelength infrared," Applied Physics Letters, Vol. 67, No. 6, August 1995)
- [6] Hassan .M.Ahmed, Msc Thesis, Measurement of Temperature Using Line width Broadening, 2009.

[7] Michael Allaby, Atmosphere: A Scientific History of Air, Weather, and Climate, (Mc Hill, New York, 2009).

[8] K. Shudiram Saha, The Earth's Atmosphere: Its Physical and Dynamic, (revised 2013).

[9] [Jack J. Lissauer](#), [Imke de Pater](#) Fundamental Planetary Science: Physics, Chemistry and Habitability, (Mc Hill, New York, 2013).

[10] [Roger G. Barry](#) & [Richard J. Chorley](#), Atmosphere. Weather and Climate, (Taylor & Francis, New York, 2010).

[11] [Paul E. Lydolph](#), Weather and Climate, (Government Institutes, United States of America, 1985).

[12] [Vincent J. Schaefer](#) & [John A. Day](#) & [Jay Pasachoff](#), A Field Guide to the Atmosphere, (Mc Hill, New York, 1998).

[13] Michael Pidwirny, Understanding Physical Geography, (University of British Columbia, 2012).

[14] [Kshudiram Saha](#), The Earth's Atmosphere, (Library of Congress, USA, 2008).

[15] [Michael Allaby](#), A Change in the Weather, (Mc Hill, New York, 2004).

[16] [Robin McLlveen](#), Fundamentals of Weather and Climate, (Oxford University Press, New York, 2010).

[17] Macmillan Publishing Co, Elements of organic chemistry, (New York, second edition, 1977).

[18] R. J. Van Zee et al, J. Am. Chem. Soc. 1988.

[19] D.H. Gibson, Chem. Rev. 96, 1996.

- [20] U. Siegentheler & J. L. Sarmiento, *Nature*, 1993,
- [21] N. Bartlett et al. *Chem. Commun.* 1996.
- [22] N. T. Nguyen & T. K. Ho, *Chem. Ber.*, *Inorganic & Organometal. Chem.*, 1996.
- [23] K. O. Karlin et al., *Inorganic Chem.*, 1994.
- [24] H. Weyl, *The Theory of Groups and Quantum Mechanics*, (Mc Hill, New York, 2000).
- [25] B. H. Bransden & G. J. Joachim, *Quantum Mechanics*, second edition, (England, 2000).
- [26] D. H. Sandiford & A. G. Phillips, *Introduction to Quantum Mechanics*, (Wiley, 2010).
- [27] [P. M. Mathews](#), [K. Venkatesan](#), *A Textbook of Quantum Mechanics*, (New Delhi, 2007).
- [28] Peter S. Riseborough, *Advanced Quantum Mechanics* (New York, 2015).
- [29] David A. B. Miller, *Quantum Mechanics for Scientists and Engineers*, (Cambridge University Press, England, 2000).
- [30] John S. Townsend, *A Modern Approach to Quantum Mechanics*, (United States of America, University Science Books, 2000)
- [31] Eric R. Bittner, *Lecture Notes on Quantum Chemistry*, (University of Houston, Department of Chemistry, 2003).
- [32] J. Michael Hollas *Modern Spectroscopy*, Fourth Edition (Wiley, England, 2004).

- [33]K . M .Haroun, PhD Thesis, Generalization of Schrodinger equation for band theory, (Sudan University of Science and Technology,Khartoum,2007).
- [34] [Walter Greiner](#), Quantum Mechanics: An Introduction, (New York ,Springer Science & Business Media, 2001).
- [35]Ashok Das & Adrian C. Melissinos ,Quantum Mechanics: A Modern Introduction,(New York, 1986).
- [36] D .law &G.Fetzer ,s .Mesropian ,Quantum interference of large organic molecules ,(Nature . com .Retrieved 2013).
- [37]Kuhn,T. s, Black body theory and the Quantum,(Oxford, clarendon press,1978).
- [38]K. Ayuel , introduction to statistical and thermal Physics, (Khartum , 2008).
- [39]R .P .Bauman , Modern Thermodynamic with statistical Mechanics , (Macmillan ,New York , 1992) .
- [40]W .C . Schieve and L . P. Horwitz , Quantum Statistical Mechanics, (Cambridge University press , New York ,2009) .
- [41] L .Schiff , Quantum Mechanics ,(Mc Graw ,Hill Book, company, Tokyo ,1968)
- [42]A . Beiser . concept of modern Physics ,(Mc Hill company ,New York ,1990) .
- [43] A . N .Matreev ,Optics ,(Mir publishers ,Moscow , 1988) .
- [44] J .Michael Holles , Modern Spectroscopy ,(University of reading ,New Delhi ,2010) .

[45] Suhair S. Makawy Suliman ,PhD Thesis,Derivation of Statistical Distributions for non Thermally Equilibrium Systems(,Sudan University of Science and Technology,Khartoum,2012).

T. C. McAlpine, et al, Pump wavelength tuning of optical pumping [46] injection cavity lasers for enhancing mid-infrared operation, Materials Research Society Symposium Proceedings,(Vol. 799, pp. Z.4.7.1-Z4.7.6., .(2004

[47]T. C. McAlpine, et al. Resonantly pumped optical pumping injection cavity lasers,(Journal of Applied Physics, Vol. 96, No. 9, November 2004).

[48] K. S. Mobarhan, Test & Characterization of Laser Diodes: Determination of Principal Parameters, (Newport Corporation).

[49]M. I. Nathan, A. B. Fowler, & G. Burns, Oscillations in Gas spontaneous emission in Fabry-Perot cavities,(Physical Review Letters, Vol. 11, No. 4, 1963).

[50]T. C. McAlpine,Cavity length study of a resonantly pumped W-OPIC semiconductor laser, (Ph.D. dissertation, University of Kansas, Lawrence, KS, 2006).

[51]M.Mahmoud,Z.Ghassemlooy and Lu Chao,Modeling And Analysis on The Thermal Tuning Of Fiber Bragg Grating For Optical Communication Applications,(U.K., 2002).

[52][Http://www.ocean.tamu.edu/education/common/notes/contents.html](http://www.ocean.tamu.edu/education/common/notes/contents.html).

[53]Edward T.Peltzer & Peter G.Brewer, Natural gas Hydrate in Oceanic and Permafrost Environments,M. D.MaxedKluwer, (Academic Publishers,Netherlands,2000).

[54] Wallace, John M. and Peter V. Hobbs. Atmospheric Science, An Introductory Survey,(Elsevier. Second Edition , 2006).

[55] Cooney, J., Measurement of Atmospheric Temperature (profile by Ramman Backscatter, J. of Apple Meteor, 1972).

56) S.W. James, M.L. Dockney, & R.P. Tatam, Simultaneous independent Temperature and strain measurement using in-fiber Bragg grating sensors Electron. Lett., vol. 32, no. 12, pp. 1133-1134, 1996)

[57] R.G. Strauth, V.E. Derr, and R. E. Cupp, Atmospheric Temperature measurement Using Ramman Backscatter, (Appl. Opt 1971).

[58] V. Bhatia & M. Vengsarcar, optical fiber long-period grating sensors, (vol. 21, no. 9, pp 692-694, 1996).

[59] A. Beiser, Concept of Modern Physics (M.C. Hill company, New York, 1990).

Ocean Optics, USB2000 Fiber Optic Spectrometer, Installation and [60] Operation Manual, Copyright 2005